

The copyright © of this thesis belongs to its rightful author and/or other copyright owner. Copies can be accessed and downloaded for non-commercial or learning purposes without any charge and permission. The thesis cannot be reproduced or quoted as a whole without the permission from its rightful owner. No alteration or changes in format is allowed without permission from its rightful owner.



**MULTIPLE SOLUTIONS AND STABILITY ANALYSIS OF
BOUNDARY LAYER FLOWS OVER A
STRETCHING/SHRINKING SHEET IN NANOFLUIDS**



SUMERA DERO

— Cd problem

Universiti Utara Malaysia

**DOCTOR OF PHILOSOPHY
UNIVERSITI UTARA MALAYSIA
2020**



Awang Had Salleh
Graduate School
of Arts And Sciences

Universiti Utara Malaysia

PERAKUAN KERJA TESIS / DISERTASI
(Certification of thesis / dissertation)

Kami, yang bertandatangan, memperakukan bahawa
(We, the undersigned, certify that)

SUMERA DERO

calon untuk Ijazah **PhD**
(candidate for the degree of)

telah mengemukakan tesis / disertasi yang bertajuk:
(has presented his/her thesis / dissertation of the following title):

“MULTIPLE SOLUTIONS AND STABILITY ANALYSIS OF BOUNDARY LAYER FLOWS OVER A STRETCHING/SHRINKING SHEET IN NANOFLUIDS”

seperti yang tercatat di muka surat tajuk dan kulit tesis / disertasi.
(as it appears on the title page and front cover of the thesis / dissertation).

Bahawa tesis/disertasi tersebut boleh diterima dari segi bentuk serta kandungan dan meliputi bidang ilmu dengan memuaskan, sebagaimana yang ditunjukkan oleh calon dalam ujian lisan yang diadakan pada : **11 Ogos 2020.**

That the said thesis/dissertation is acceptable in form and content and displays a satisfactory knowledge of the field of study as demonstrated by the candidate through an oral examination held on: August 11, 2020.

Pengerusi Viva:
(Chairman for VIVA)

Assoc. Prof. Dr. Rahela Abdul Rahim

Tandatangan
(Signature)

Pemeriksa Luar:
(External Examiner)

Assoc. Prof. Dr. Nor Fadzillah Mohd Mokhtar

Tandatangan
(Signature)

Pemeriksa Dalam:
(Internal Examiner)

Dr. Teh Yuan Ying

Tandatangan
(Signature)

Nama Penyelia/Penyelia-penyelia:
(Name of Supervisor/Supervisors)

Dr. Azizah Mohd Rohni

Tandatangan
(Signature)

Nama Penyelia/Penyelia-penyelia:
(Name of Supervisor/Supervisors)

Assoc. Prof. Dr. Azizan Saaban

Tandatangan
(Signature)

Tarikh:
(Date) **August 11, 2020**

Permission to Use

In presenting this thesis in fulfilment of the requirements for a postgraduate degree from Universiti Utara Malaysia, I agree that the Universiti Library may take it freely available for inspection. I further agree that permission for the copying of this thesis in any manner, in whole or in part, for scholarly purpose may be granted by my supervisor(s) or, in their absence, by the Dean of Awang Had Salleh Graduate School of Arts and Sciences. It is understood that any copying or publication or use of this thesis or parts thereof for financial gain shall not be allowed without my written permission. It is also understood that due recognition shall be given to me and to Universiti Utara Malaysia for any scholarly use which may be made of any material from my thesis.

Requests for permission to copy or to make other use of materials in this thesis, in whole or in part, should be addressed to:

Dean of Awang Had Salleh Graduate School of Arts and Sciences
UUM College of Arts and Sciences Malaysia
Universiti Utara Malaysia
06010 UUM Sintok

Abstrak

Kajian mengenai penyelesaian berbilang pada aliran lapisan sempadan telah menjadi tumpuan dalam bidang dinamik bendalir sejak kebelakangan ini. Sehubungan itu, analisis kestabilan juga penting untuk mengenal pasti penyelesaian stabil dan tak stabil. Dalam tesis ini, kemungkinan berlakunya penyelesaian berbilang telah dikaji untuk aliran lapisan sempadan atas helaian meregang/mengecut dalam bendalir nano. Lima masalah berbeza telah dipertimbangkan yang mana dua masalah menggunakan model bendalir nano yang dicadangkan oleh Buongiorno dan tiga masalah yang lain menggunakan model bendalir nano yang dicadangkan oleh Tiwari dan Das. Bendalir asas yang dipertimbangkan dalam kajian ini adalah bendalir likat, bendalir Casson dan bendalir mikro kutub. Model matematik yang menakluk aliran lima masalah yang berbeza telah dibina. Penjelmaan keserupaan telah digunakan untuk menjelmakan persamaan menakluk dalam bentuk persamaan pembezaan separa kepada persamaan pembezaan biasa tak linear. Sistem yang terhasil kemudiannya diselesaikan secara berangka menggunakan kaedah menembak dengan bantuan fungsi *shootlib* dalam perisian Maple. Bagi mengesahkan keputusan yang diperoleh dalam kajian ini, perbandingan untuk kes tertentu telah dibuat dan menepati penyelesaian yang ada dalam kajian lepas. Daripada kajian ini, didapati bahawa peningkatan parameter sedutan akan meningkatkan kadar pemindahan haba dalam kedua-dua kes regangan dan pengecutan. Walau bagaimanapun, ianya mengakibatkan kadar geseran kulit menurun untuk kes regangan tetapi meningkat untuk kes pengecutan. Seterusnya, parameter sedutan, parameter Casson dan nombor Biot menurunkan profil suhu manakala parameter radiasi, gerakan Brownian dan termoforesis menyumbang kepada sebaliknya. Keputusan juga menunjukkan berlakunya penyelesaian berbilang dalam kesemua masalah yang dipertimbangkan. Oleh itu, analisis kestabilan telah dilakukan untuk mengenal pasti kestabilan penyelesaian berbilang dengan menggunakan penyelesai *bvp4c* dalam perisian Matlab. Analisis kestabilan menunjukkan bahawa penyelesaian pertama adalah stabil sementara penyelesaian kedua dan ketiga adalah tidak stabil.

Kata Kunci: Aliran lapisan sempadan, Bendalir nano, Penyelesaian berbilang, Analisis kestabilan, Helaian meregang/mengecut.

Abstract

Studies of multiple solutions on boundary layer flows have gained much attention in the field of fluid dynamics in the recent years. In this regard, stability analysis is also important to identify the stable and unstable solutions. In this thesis, the possibility of occurrence of multiple solutions has been studied for boundary layer flows over stretching/shrinking sheet in nanofluids. Five different problems have been considered where two of the problems used nanofluid model proposed by Buongiorno and the remaining three problems used nanofluid model proposed by Tiwari and Das. The base fluids considered in this study are viscous fluid, Casson fluid and micropolar fluid. The mathematical models which govern the flows of five different problems have been constructed. Similarity transformations have been employed to transform the governing equations of partial differential equations to nonlinear ordinary differential equations. The resulting system is then solved numerically using shooting method with the aid of *shootlib* function in Maple software. To validate the results obtained in this study, comparison for specific cases have been done and in good agreement with existing solutions in literature. From this study, it is found that an increase of suction parameters will increase the rate of heat transfer in both stretching and shrinking cases. However, it causes the rate of skin friction to decrease for stretching case but to increase for shrinking case. Further, suction parameter, Casson parameter and Biot number decrease the temperature profiles but radiation, Brownian motion and thermophoresis parameters contribute towards the opposite. The results also displayed the occurrence of multiple solutions in all the problems considered. Therefore, the stability analysis has been performed to identify the stability of multiple solutions by using *bvp4c* solver in Matlab. The stability analysis indicates that the first solution is stable while the second and third solutions are unstable.

Keywords: Boundary layer flows, Nanofluid, Multiple solutions, Stability analysis, Stretching/Shrinking Sheet.

Acknowledgements

Bismillahirrahmanirrahim

First and foremost, praise to the Almighty Allah, whom ultimately we depend on for sustenance and guidance. My sincere and profound appreciation goes to my supervisors, Dr. Azizah Mohd Rohni and Associate Prof. Dr. Azizan Saaban, for their guidance, support, encouragement and constructive comments during my study. They were always there for me whenever I needed their help or advice.

I am deeply grateful to my family for their unconditional trust, encouragement, and supplications throughout this journey that was the source of my strength and perseverance.

My special thanks and appreciation to my loving and kind husband, Liaquat, and my beautiful kids, Balach and Zunaira Fatima. Their sacrifices, love and understanding really motivated me to work harder in completing this thesis. May Allah bless them all.

I would like to thank Universiti Utara Malaysia for giving me chances to study in this beautiful university. My appreciation also goes to administrative staffs in Awang Had Salleh Graduate School and School of Quantitative Sciences, UUM for being helpful and supportive during my study here.

Last but not least, I would like to thank University of Sindh, Pakistan for assisting me with study leave and financial support.

Table of Contents

Permission to Use	ii
Abstrak	iii
Abstract	iv
Acknowledgements	v
Table of Contents	vi
List of Tables	x
List of Figures	xiv
List of Abbreviations	xx
List of Appendices	xxiv
CHAPTER ONE INTRODUCTION	1
1.1 Introduction	1
1.2 Nanofluid	1
1.2.1 Nanofluid Models	3
1.2.1.1 Buongiorno Model (2006)	4
1.2.1.2 Tiwari and Das Model (2007)	4
1.2.2 Base Fluid	5
1.2.2.1 Viscous Fluid	5
1.2.2.2 Casson Fluid	6
1.2.2.3 Micropolar Fluid	6
1.3 Boundary Layer Theory	7
1.3.1 Velocity Boundary Layer	7
1.3.2 Thermal Boundary Layer	8
1.3.3 Concentration Boundary Layer	9
1.4 Dimensionless Quantities	10
1.4.1 Reynolds number	10
1.4.2 Prandtl Number	11
1.4.3 Grashof Number	12
1.4.4 Eckert Number	12
1.4.5 Radiation Parameter	13
1.4.6 Porosity Parameter	13
1.4.7 Heat Source/Sink Parameter	13

1.4.8	Schmidt Number	14
1.4.9	Skin Friction.....	14
1.4.10	Nusselt Number.....	14
1.4.11	Sherwood Number.....	15
1.4.12	Mixed Convection Parameter.....	15
1.4.13	Biot Number.....	16
1.5	Problem Statement.....	16
1.6	Research Questions	17
1.7	Objectives and Scope of the Study.....	18
1.8	Research Methodology	19
1.8.1	Research Methodology.....	19
1.8.2	Mathematical Analysis	19
1.8.3	Numerical Computation	19
1.8.3.1	Shooting Method (<i>shootlib</i> function in Maple).....	20
1.8.3.2	Three stage Lobatto IIIa formula (<i>bvp4c</i> solver in Matlab).....	21
1.9	Significance of the Study.....	22
1.10	Thesis Organization.....	23
CHAPTER TWO LITERATURE REVIEW		26
2.1	Introduction	26
2.2	Boundary Layer Flow over Shrinking/Stretching Surface in Nanofluids	26
2.3	Boundary Layer Flow of Viscous Nanofluid	28
2.4	Boundary Layer Flow of Casson Nanofluid.....	32
2.5	Boundary Layer Flow of Micropolar Nanofluid	35
2.6	Multiple Similarity Solutions and Stability Analysis.....	37
CHAPTER THREE GOVERNING EQUATIONS.....		41
3.1	Introduction	41
3.2	Nanofluid Model Proposed by Buongiorno (2006).....	41
3.3	Nanofluid Model Proposed by Tiwari and Das (2007).....	44
3.4	Casson Nanofluid Flow using Buongiorno's Model	46
3.5	Boundary Layer Scale Analysis	49
3.6	Boundary Layer Flow of Micropolar Fluid.....	54
3.7	Viscous and Casson Nanofluid using Tiwari and Das's Model.....	56

CHAPTER FOUR BOUNDARY LAYER FLOW OF CASSON NANOFUID OVER PERMEABLE STRETCHING/SHRINKING SHEET WITH VISCOUS DISSIPATION AND CHEMICAL REACTION: BUONGIORNO'S MODEL..58

4.1	Introduction	58
4.2	Mathematical Formulation	59
4.3	Similarity Transformation	60
4.4	Stability Analysis.....	62
4.5	Numerical Method.....	65
4.6	Results and Discussion	65
4.7	Conclusions	87

CHAPTER FIVE BOUNDARY LAYER FLOW OF MICROPOLAR NANOFUID OVER STRETCHING/SHRINKING SHEET WITH SUCTION AND SLIP EFFECTS: BUONGIORNO'S MODEL.....89

5.1	Introduction	89
5.2	Mathematical Formulation	90
5.3	Similarity Transformation	91
5.4	Stability Analysis.....	93
5.5	Numerical Method.....	96
5.6	Results and Discussion	97
5.7	Conclusions	115

CHAPTER SIX BOUNDARY LAYER FLOW OF CASSON NANOFUID OVER STRETCHING/SHRINKING SHEET WITH EFFECT OF POROSITY AND VISCOUS DISSIPATION: TIWARI AND DAS'S MODEL..... 117

6.1	Introduction	117
6.2	Mathematical Formulation	118
6.3	Similarity Transformation	120
6.4	Stability Analysis.....	121
6.5	Numerical Method.....	124
6.6	Results and Discussion	124
6.7	Conclusions	147

CHAPTER SEVEN BOUNDARY LAYER FLOW OF VISCOUS NANOFUID OVER PERMEABLE EXPONENTIALLY SHRINKING SHEET: TIWARI AND DAS'S MODEL	149
7.1 Introduction	149
7.2 Mathematical Formulation	150
7.3 Similarity Transformation	151
7.4 Stability Analysis.....	153
7.5 Numerical Method.....	155
7.6 Results and Discussion	155
7.7 Conclusions	175
CHAPTER EIGHT BOUNDARY LAYER FLOW OF CASSON NANOFUID OVER A PERMEABLE EXPONENTIALLY SHRINKING/STRETCHING SHEET: TIWARI AND DAS'S MODEL.....	176
8.1 Introduction	176
8.2 Mathematical Formulation	177
8.3 Similarity Transformation.....	178
8.4 Stability Analysis.....	179
8.5 Numerical Method.....	182
8.6 Results and Discussion	183
8.7 Conclusions	203
CHAPTER NINE CONCLUSIONS.....	205
9.1 Summary of Research.....	205
9.2 Suggestions for Future Research.....	211
REFERENCES.....	212
APPENDIX A.....	224
APPENDIX B.....	238
APPENDIX C.....	255
APPENDIX D.....	259
APPENDIX E.....	263
APPENDIX F.....	276

List of Tables

Table 4.1 The value of $-\theta'(0)$ for different value Prandtl number Pr when $\lambda=1, S=0$ in absence of Ec, Nb, Ni and Bi	66
Table 4.2 The smallest eigenvalue ε for different values of S, β and λ	67
Table 4.3 Variation of $f'(0), -\theta'(0)$ and $-\Phi'(0)$ with λ for the first and second solutions when $\beta=2.5, Pr=Sc=1, \delta=Ec=K_1=0.1, Ni=\xi=0.5, Bi=5, Nb=0.3$ and $S=2.3$	70
Table 4.4 Variation of $f'(0), -\theta'(0)$ and $-\Phi'(0)$ for with λ the first and second solutions when $\beta=2.5, Pr=Sc=1, \delta=Ec=K_1=0.1, Ni=\xi=0.5, Bi=5, Nb=0.3$, and $S=2.4$	70
Table 4.5 Variation of $f'(0), -\theta'(0)$ and $-\Phi'(0)$ with λ for the first and second solutions when $\beta=2.5, Pr=Sc=1, \delta=Ec=K_1=0.1, Ni=\xi=0.5, Bi=5, Nb=0.3$, and $S=2.6$	71
Table 4.6 Variation of $f'(0), -\theta'(0)$ and $-\Phi'(0)$ with S for the first and second solutions when $Pr=Sc=1, \delta=Ec=K_1=0.1, \lambda=-1, Ni=\xi=0.5, Bi=5, Nb=0.3$, and $\beta=\infty$	74
Table 4.7 Variation $f'(0), -\theta'(0)$ and $-\Phi'(0)$ with S for the first and second solutions when $Pr=Sc=1, \delta=Ec=K_1=0.1, \lambda=-1, Ni=\xi=0.5, Bi=5, Nb=0.3$, and $\beta=0.5$	74
Table 4.8 Variation of $f'(0), -\theta'(0)$ and $-\Phi'(0)$ with S for the first and second solutions when $Pr=Sc=1, \delta=Ec=K_1=0.1, \lambda=-1, Ni=\xi=0.5, Bi=5, Nb=0.3$, and $\beta=2.5$	75
Table 5.1 Comparative results for surface drag force $(C_f(Re_x)^{1/2})$ for various values of $m = 0, 0.5$ for micropolar fluid with (Hayat <i>et al.</i> 2017) for the various values of K at $\lambda=1$ and $S=0$	98
Table 5.2 Smallest eigenvalues for different values of K and S	99
Table 5.3 Variation of $f'(0), g'(0), -\theta'(0)$ and $-\Phi'(0)$ with λ for the first and second solutions when $Pr=K=Sc=1, Rd=Nb=0.2, Bi=5, Ni=0.5, \delta=\delta_r=\delta_c=0.1$, and $S=2.8$	102
Table 5.4 Variation of $f'(0), g'(0), -\theta'(0)$ and $-\Phi'(0)$ with λ for the first and second solutions when $Pr=K=Sc=1, Rd=Nb=0.2, Bi=5, Ni=0.5, \delta=\delta_r=\delta_c=0.1$, and $S=3$	103

Table 5.5 Variation of $f''(0)$, $g'(0)$, $-\theta'(0)$ and $-\phi'(0)$ with λ for the first and second solutions when $Pr=K=Sc=1, Rd=N_b=0.2, Bi=5, N_t=0.5$ $\delta= \delta_T= \delta_C=0.1$, and $S=3.2$	103
Table 5.6 Variation of $f''(0)$, $g'(0)$, $-\theta'(0)$ and $-\phi'(0)$ with S for the first and second solutions when $Pr=Sc=1, \lambda=-1, Rd=N_b=0.2, Bi=5, N_t=0.5$ $\delta= \delta_T= \delta_C=0.1$, and $K=0.107$	107
Table 5.7 Variation of $f''(0)$, $g'(0)$, $-\theta'(0)$ and $-\phi'(0)$ with S for the first and second solutions when $Pr=Sc=1, \lambda=-1, Rd=N_b=0.2, Bi=5, N_t=0.5$ $\delta= \delta_T= \delta_C=0.1$, and $K=1.107$	107
Table 5.8 Variation of $f''(0)$, $g'(0)$, $-\theta'(0)$ and $-\phi'(0)$ with S for the first and second solutions when $Pr=Sc=1, \lambda=-1, Rd=N_b=0.2, Bi=5, N_t=0.5$ $\delta= \delta_T= \delta_C=0.1$, and $K=2$	108
Table 6.1 Thermo physical properties of the Casson fluid and the nanoparticles (Hatami and Ganji, 2014; Lund, Omar, Khan, & Dero, 2019).....	119
Table 6.2 Comparison of results for $f''(0)$ and $-\theta'(0)$ for $Pr=0.7, \lambda=-1, Ec=0$, and $\phi=0$	126
Table 6.3 Smallest eigenvalues ε for the first and second solutions at different values of S, β and K_I for Cu and Ag nanoparticles when $Pr=10, \lambda=-1, Ec=0.5$ and $\phi=0.1$	126
Table 6.4 Variation of $f''(0)$ and $-\theta'(0)$ with λ for the first and second solutions when $Pr=10, Ec=0.5, K_I=0.5, \beta=2, \phi=0.1$ and $S=2$ for Nanoparticle (Silver Ag)	128
Table 6.5 Variation of $f''(0)$ and $-\theta'(0)$ with λ for the first and second solutions when $Pr=10, Ec=0.5, K_I=0.5, \beta=2, \phi=0.1$ and $S=2.4$ for Nanoparticle (Silver Ag)	129
Table 6.6 Variation of $f''(0)$ and $-\theta'(0)$ with λ for the first and second solutions when $Pr=10, Ec=0.5, K_I=0.5, \beta=2, \phi=0.1$ and $S=2.8$ for Nanoparticle (Silver Ag)	129
Table 6.7 Variation of $f''(0)$ and $-\theta'(0)$ with λ for the first and second solutions when $Pr=10, Ec=0.5, K_I=0.5, \beta=2, \phi=0.1$ and $S=2$ for Nanoparticle (Copper Cu).	131
Table 6.8 Variation of $f''(0)$ and $-\theta'(0)$ with λ for the first and second solutions when $Pr=10, Ec=0.5, K_I=0.5, \beta=2, \phi=0.1$ and $S=2.4$ for Nanoparticle (Copper Cu).....	132

Table 6.9 Variation of $f''(0)$ and $-\theta'(0)$ with λ for the first and second solutions when $Pr=10$, $Ec=0.5$, $K_1=0.5$, $\beta=2$, $\phi=0.1$ and $S=2.8$ for Nanoparticle (Copper Cu).....	132
Table 6.10 Variation of $f''(0)$ and $-\theta'(0)$ with S for the first and second solutions when $Pr=10$, $Ec=0.5$, $K_1=0.5$, $\beta=2$, $\lambda=-1$ and $\phi=0$ for Nanoparticle (Silver Ag).	134
Table 6.11 Variation of $f''(0)$ and $-\theta'(0)$ with S for the first and second solutions when $Pr=10$, $Ec=0.5$, $K_1=0.5$, $\beta=2$, $\lambda=-1$ and $\phi=0.1$ for Nanoparticle (Silver Ag)	135
Table 6.12 Variation of $f''(0)$ and $-\theta'(0)$ with S for the first and second solutions when $Pr=10$, $Ec=0.5$, $K_1=0.5$, $\beta=2$, $\lambda=-1$ and $\phi=0.2$ for Nanoparticle (Silver Ag).	135
Table 6.13 Variation of $f''(0)$ and $-\theta'(0)$ with S for the first and second solutions when $Pr=10$, $Ec=0.5$, $K_1=0.5$, $\beta=2$, $\lambda=-1$ and $\phi=0$ for Cu.....	137
Table 6.14 Variation of $f''(0)$ and $-\theta'(0)$ with S for the first and second solutions when $Pr=10$, $Ec=0.5$, $K_1=0.5$, $\beta=2$, $\lambda=-1$ and $\phi=0.1$ for Cu.....	138
Table 6.15 Variation of $f''(0)$ and $-\theta'(0)$ with S for the first and second solutions when $Pr=10$, $Ec=0.5$, $K_1=0.5$, $\beta=2$, $\lambda=-1$ and $\phi=0.2$ for Cu.....	138
Table 7.1 The thermo-physical properties of nanoparticles and water (Mutuku-Njane, 2014).....	156
Table 7.2 The comparison of the values of heat transfer rate $-\theta'(0)$ for various values of Pr	156
Table 7.3 The obtained smallest eigenvalues ε at various values of δ_T and δ for Cu, Ag and Al nanoparticles when $Pr=6.2$, $Rd=0.2$, $\phi=0.1$ and $\lambda=-1$	157
Table 7.4 Value of the critical points of investigated nanofluids	158
Table 7.5 Variation of $f''(0)$ and $-\theta'(0)$ with S for the first and second solutions when $Pr=6.2$, $\delta=0.1$, $\delta_T=0.1$, $Rd=0.2$, $\lambda=-1$ and $\phi=0$ for Cu.....	160
Table 7.6 Variation of $f''(0)$ and $-\theta'(0)$ with S for the first and second solutions when $Pr=6.2$, $\delta=0.1$, $\delta_T=0.1$, $Rd=0.2$, $\lambda=-1$ and $\phi=0.1$ for Cu.....	160
Table 7.7 Variation of $f''(0)$ and $-\theta'(0)$ with S for the first and second solutions when $Pr=6.2$, $\delta=0.1$, $\delta_T=0.1$, $Rd=0.2$, $\lambda=-1$ and $\phi=0.2$ for Cu.....	161

Table 7.8 Variation of $f''(0)$ and $-\theta'(0)$ with S for the first and second solutions when $Pr=6.2, \delta=0.1, \delta_T=0.1, Rd=0.2, \lambda=-1$ and $\phi=0$ for Ag.....	164
Table 7.9 Variation of $f''(0)$ and $-\theta'(0)$ with S for the first and second solutions when $Pr=6.2, \delta=0.1, \delta_T=0.1, Rd=0.2, \lambda=-1$ and $\phi=0.1$ for Ag.....	164
Table 7.10 Variation of $f''(0)$ and $-\theta'(0)$ with S for the first and second solutions when $Pr=6.2, \delta=0.1, \delta_T=0.1, Rd=0.2, \lambda=-1$ and $\phi=0.2$ for Ag.....	165
Table 7.11 Variation of $f''(0)$ and $-\theta'(0)$ with S for the first and second solutions when $Pr=6.2, \delta=0.1, \delta_T=0.1, Rd=0.2, \lambda=-1$ and $\phi=0$ for Al.....	165
Table 7.12 Variation of $f''(0)$ and $-\theta'(0)$ with S for the first and second solutions when $Pr=6.2, \delta=0.1, \delta_T=0.1, Rd=0.2, \lambda=-1$ and $\phi=0.1$ for Al.....	166
Table 7.13 Variation of $f''(0)$ and $-\theta'(0)$ with S for the first and second solutions when $Pr=6.2, \delta=0.1, \delta_T=0.1, Rd=0.2, \lambda=-1$ and $\phi=0.2$ for Al.....	166
Table 8.1 Thermo physical properties of the Casson fluid and the nanoparticles (Hatami and Ganji, 2014; Lund, Omar, Khan, & Dero, 2019).....	184
Table 8.2 Comparative results of the first solution for skin friction coefficient $f''(0)$ and the Local Nusselt number $-\theta'(0)$ for various values of Pr at $\lambda=Rd=1, \beta \rightarrow \infty$ and $\phi=S=\zeta=\chi=\delta=\delta_T=0$	184
Table 8.3 The smallest eigenvalues for different values of the parameters β, λ and S for $Pr=1.5, \delta=0.1, \delta_T=0.1, \phi=0.1, \chi=0.1, \zeta=1$ and $Rd=0.5$	186
Table 8.4 Variation of $f''(0)$ and $-\theta'(0)$ with λ for Graphite Oxide nanoparticle when $Pr=1.5, \zeta=1, \delta_T=0.2, Rd=0.5, \beta=2.5,$ and $\phi=\chi=\delta=0.1$	191

List of Figures

Figure 1.1 Velocity Boundary Layer	8
Figure 1.2 Thermal Boundary Layers.....	9
Figure 1.3 Concentration Boundary Layer	10
Figure 1.4 Flow chart of research methodology	21
Figure 4.1 Coordinate system and physical model	59
Figure 4.2 The variation of the skin friction coefficient $f''(0)$ along λ for the several values of S	69
Figure 4.3 The variation of the Nusselt number $-\theta'(0)$ along λ for the several values of S	69
Figure 4.4 The variation of the rate of Sherwood numbers $-\phi'(0)$ along λ for the several values of S	69
Figure 4.5 The variation of the skin friction coefficient $f''(0)$ along S for the several values of β	72
Figure 4.6 The variation of the rate of heat transfer $-\theta'(0)$ along S for the several values of β	73
Figure 4.7 The variation of the rate of concentration $-\phi'(0)$ along S for the several values of β	73
Figure 4.8 The velocity profile $f'(\eta)$ for the several values of β	76
Figure 4.9 The temperature profile $\theta(\eta)$ for the several values of β	76
Figure 4.10 The concentration profile $\phi(\eta)$ for the several values of β	77
Figure 4.11 The velocity profile $f'(\eta)$ for the several values of K_1	78
Figure 4.12 The velocity profile $f'(\eta)$ for the several values of S	78
Figure 4.13 The temperature profile $\theta(\eta)$ for the several of S	79
Figure 4.14 The concentration profile $\phi(\eta)$ for the several values S	80
Figure 4.15 The temperature profile $\theta(\eta)$ for the several values of Pr	80

Figure 4.16 The temperature profiles $\theta(\eta)$ for the several values of N_b	81
Figure 4.17 The temperature profile $\theta(\eta)$ for the several values of N_t	82
Figure 4.18 The concentration profile $\phi(\eta)$ for the several values of N_b	83
Figure 4.19 The concentration profile $\phi(\eta)$ for the several values of N_t	83
Figure 4.20 The temperature profile $\theta(\eta)$ for the several values of Ec	84
Figure 4.21 The concentration profile $\phi(\eta)$ for the several values of Sc	85
Figure 4.22 The temperature profile $\theta(\eta)$ for the several values of Bi	85
Figure 4.23 The concentration profile $\phi(\eta)$ for the several values of Bi	86
Figure 4.24 The concentration profile $\phi(\eta)$ for the several values of ξ	87
Figure 5.1 Geometry of flow problem and coordinate system	90
Figure 5.2 The coefficient of skin friction with different values of S with variation of λ	100
Figure 5.3 The coefficient of couple stress with different values of S with variation of λ	101
Figure 5.4 The heat transfer rate with different values of S with variation of λ	101
Figure 5.5 The concentration transfer rate with different values of S with variation of λ	102
Figure 5.6 The coefficient of skin friction with different values of K with variation of S	105
Figure 5.7 The coefficient of couple stress with different values K with variation of S	105
Figure 5.8 The heat transfer rate with different values K with variation of S	106
Figure 5.9 The concentration transfer rate with different values K with variation of S	106
Figure 5.10 The velocity profile for the various values of the K	109
Figure 5.11 The velocity profile for the various values of the δ	109

Figure 5.12 The microrotation profile for the various values of m	110
Figure 5.13 The microrotation profile for the various values of K	111
Figure 5.14 The temperature profile for the various values of K	111
Figure 5.15 The temperature profile for the various values of N_t	112
Figure 5.16 The temperature profile for the various values of N_b	113
Figure 5.17 The temperature profile for the various values of δ_T	113
Figure 5.18 The concentration profile for the various values of N_t	114
Figure 5.19 The concentration profile for the various values of N_b	115
Figure 5.20 The concentration profile for the various values of δ_C	115
Figure 6.1 Physical model of flow.....	118
Figure 6.2 Graph of $f''(0)$ with different values of λ and S for Ag-C ₆ H ₉ NaO ₇ nanofluid	127
Figure 6.3 Graph of $-\theta'(0)$ with different values of λ and S for Ag-C ₆ H ₉ NaO ₇ nanofluid	128
Figure 6.4 Graph of $f''(0)$ with different values for λ and S for Cu-C ₆ H ₉ NaO ₇ nanofluid	130
Figure 6.5 Graph of $-\theta'(0)$ with different values of λ and S for Cu-C ₆ H ₉ NaO ₇ nanofluid	131
Figure 6.6 Graph of $f''(0)$ with different values of suction S for different values of ϕ in Ag-C ₆ H ₉ NaO ₇ nanofluid	133
Figure 6.7 Graph of rate of heat transfer $-\theta'(0)$ with different values of suction S for different values of ϕ in Ag-C ₆ H ₉ NaO ₇ nanofluid.....	134
Figure 6.8 $f''(0)$ with different values of suction S for different values of ϕ Cu- C ₆ H ₉ NaO ₇ nanofluid	136
Figure 6.9 Rate of heat transfer $-\theta'(0)$ with different values of suction S for different values of ϕ is Cu-C ₆ H ₉ NaO ₇ nanofluid	137
Figure 6.10 Heat transfer rate with different values of ϕ in Cu-C ₆ H ₉ NaO ₇ and Ag- C ₆ H ₉ NaO ₇ nanofluid	139

Figure 6.11 Skin frictions coefficient with different values of ϕ in Cu-C ₆ H ₉ NaO ₇ and Ag-C ₆ H ₉ NaO ₇ nanofluid	140
Figure 6.12 Effect of β on the velocity distributions for Cu-C ₆ H ₉ NaO ₇ nanofluid ...	141
Figure 6.13 Effect of β on the velocity distributions for Ag-C ₆ H ₉ NaO ₇ nanofluid ...	141
Figure 6.14 The combined effect of β on the velocity distribution for Cu and Ag-C ₆ H ₉ NaO ₇ nanofluid	142
Figure 6.15 Effect of β on the temperature distribution for Cu-C ₆ H ₉ NaO ₇ nanofluid	143
Figure 6.16 Effect of β on the temperature distribution for Ag-C ₆ H ₉ NaO ₇ nanofluid	144
Figure 6.17 The combined effect of β on the temperature distribution for Cu and Ag	144
Figure 6.18 Effect of Ec on the temperature distribution for Cu-C ₆ H ₉ NaO ₇ nanofluid	145
Figure 6.19 Effect of Ec on the temperature distribution for Ag-C ₆ H ₉ NaO ₇ nanofluid	146
Figure 6.20 Effect of Pr on the temperature distribution for Cu-C ₆ H ₉ NaO ₇ nanofluid	146
Figure 6.21 Effect of Pr on the temperature distribution for Ag-C ₆ H ₉ NaO ₇ nanofluid	147
Figure 7.1 Geometry of flow problem and coordinate system	150
Figure 7.2 The variation of $f''(0)$ with S at different values of ϕ for the Cu-water based nanofluid	159
Figure 7.3 The variation of $-\theta'(0)$ with S at different values of ϕ for the Cu-water based nanofluid	159
Figure 7.4 The variation of $f''(0)$ with S at different values of ϕ for the Ag-water based nanofluid	162
Figure 7.5 The variation of $-\theta'(0)$ with S at different values of ϕ for the Ag-water based nanofluid	162

Figure 7.6 The variation of $f''(0)$ along S at different values of ϕ for the Al-water based nanofluid	163
Figure 7.7 The variation of $-\theta'(0)$ with S at different values of ϕ for the Al-water based nanofluid	163
Figure 7.8 The variation of skin friction coefficient with ϕ for the used specific nanoparticles	168
Figure 7.9 The variation of the local Nusselt number along the ϕ for the used specific nanoparticles	168
Figure 7.10 Velocity profiles $f'(\eta)$ for different values of ϕ for different nanoparticles	169
Figure 7.11 Temperature profiles $\theta(\eta)$ for different values of ϕ for different nanoparticles	169
Figure 7.12 Velocity profiles $f'(\eta)$ for Cu-water nanofluid for different values of velocity slip δ	170
Figure 7.13 The velocity profiles $f'(\eta)$ for Ag-water nanofluid at the different values of velocity slip δ	171
Figure 7.14 The temperature profiles $\theta(\eta)$ for Cu-water nanofluid for Rd	172
Figure 7.15 The temperature profiles $\theta(\eta)$ of the Ag-water for Rd	173
Figure 7.16 The temperature profiles $\theta(\eta)$ of the Al-water nanofluid at different values of thermal radiation Rd	173
Figure 7.17 The temperature profiles $\theta(\eta)$ of the Ag-water nanofluid for δ_T	174
Figure 7.18 The temperature profiles $\theta(\eta)$ of the Al-water nanofluid for δ_T	174
Figure 8.1 Physical model of flow	177
Figure 8.2 Skin friction coefficient of Cu with variation of the λ for different values of S	187
Figure 8.3 Skin friction coefficient of Al with variation of λ for different values of S	187
Figure 8.4 Skin friction coefficient of GO with variation of λ for different values of S	188

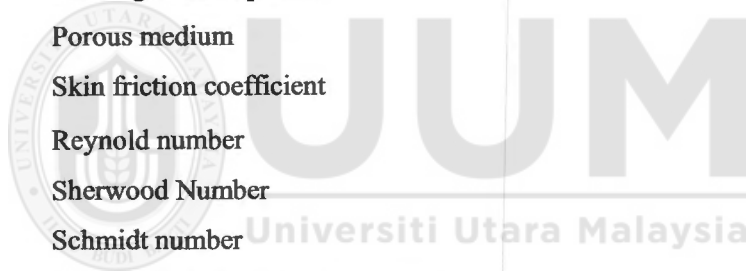
Figure 8.5 Local Nusselt number of Cu with variation of λ for different values of S	189
Figure 8.6 Local Nusselt number of Al with variation of λ for different values of S	189
Figure 8.7 Local Nusselt number of GO with variation of λ for different values of S	190
Figure 8.8 The effects of the different nanoparticles on $f''(0)$	192
Figure 8.9 The differentiation in influence between different nanoparticles on $-\theta'(0)$	192
Figure 8.10 The differentiation between effects of the different nanoparticles on $f'(\eta)$	193
Figure 8.11 The differentiation between effects of the different nanoparticles on $\theta(\eta)$	194
Figure 8.12 The velocity profile $f'(\eta)$ for different values of β	195
Figure 8.13 The velocity profile $f'(\eta)$ for different values of ζ	196
Figure 8.14 The velocity profile $f'(\eta)$ for different values of δ	197
Figure 8.15 The velocity profile $f'(\eta)$ for different values of ϕ	198
Figure 8.16 The temperature profile $\theta(\eta)$ for different values of ϕ	198
Figure 8.17 The velocity profile $f'(\eta)$ for different values of S	199
Figure 8.18 The temperature profile $\theta(\eta)$ for different values of S	200
Figure 8.19 The temperature profile $\theta(\eta)$ for different values of Pr	201
Figure 8.20 The temperature profile $\theta(\eta)$ for different values of Rd	201
Figure 8.21 The temperature profile $\theta(\eta)$ for different values of δ_r	202
Figure 8.22 The temperature profile $\theta(\eta)$ for different values of χ	203

List of Abbreviations

Roman letters

(x, y)	Cartesian coordinates along the sheet and normal to it, respectively
(u, v)	Velocity component in Cartesian coordinate
N	Micromotional or angular velocity of fluid
T	Fluid temperature
T_w	Sheet temperature
T_∞	Ambient fluid temperature
C	Nanoparticle volumetric fraction
C_w	Concentration of nanoparticles at sheet
C_∞	Concentration of nanoparticles of ambient fluid
U_∞	Constant free stream velocity of the fluid
U_w	characteristic velocity of the sheet,
u_w	Velocity of the shrinking/stretching sheet
v_w	Velocity of the mass transfer/suction
D_T	Coefficient of thermophoretic diffusion
D_B	Coefficient of Brownian diffusion
P	Fluid pressure
k_{nf}	thermal conductivity of the nanofluid
$C_6H_9NaO_7$	Sodium alginate
Ag	Silver
Al	Aluminium
Al_2O_3	Alumina
Cu	Copper
CuO	Copper oxide
GO	Graphite oxide
TiO_2	Titanium dioxide
f	non-dimensional stream function
f'	Dimensionless velocity
L	characteristic length of the sheet

T_0	characteristic temperature of the sheet
Bi	Biot number
$^{\circ}C$	Centigrade
N_t	Thermophoresis parameter
N_b	Brownian motion parameter
Ec	Eckert number
Gr	Grashof Number
g	Gravitational acceleration
K^*	Heat mean absorption coefficient
Nu_x	Nusselt number
O	Order
$\%$	Percentage
∇	Del or gradient operator
K	Porous medium
C_f	Skin friction coefficient
Re_x	Reynold number
Sh_x	Sherwood Number
Sc	Schmidt number
C_p	Specific heat at constant pressure
S	Suction/Injection parameter
Rd	Thermal radiation
V	Velocity vector
P_y	Yield stress of fluid
C_p	Specific heat at constant pressure
S	Suction/Injection parameter
Pr	Prandtl Number



Greek letters

α	thermal diffusivity of the fluid
α_{nf}	coefficient of thermal expansion
μ	dynamic viscosity of the fluid
μ_{nf}	effective dynamic viscosity of the nanofluid
μ_B	Plastic dynamical viscosity
ρ	Density of fluid
ρ_{nf}	effective density of the nanofluid
χ	Source/sink parameter
τ_w	Ratio between the effective heat capacity of the Nanoparticle and fluid
β_T	Coefficient of thermal expansion
$(\rho C_p)_{nf}$	heat capacitance of the nanofluid
η	Similarity variable
τ	Time dependent similarity variable
κ	Vortex viscosity of fluid
κ_1	Porosity parameter
ε	Unknown eigenvalue parameter
ε_1	Smallest eigenvalue parameter
ζ	mixed convection/buoyancy parameter
γ^*	Spin gradient viscosity
σ^*	Stefan–Boltzman constant
ϑ	kinematic viscosity of the fluid
ψ	stream function
θ	dimensionless temperature
ϕ	nanoparticle volume fraction
$-\theta'(0)$	Local Nusselt number
$-\phi'(0)$	Local Sherwood number
ξ	Dimensionless chemical reaction parameter
λ	stretching/shrinking parameter

Subscripts

w	condition at the surface
∞	free stream/ambient condition
f	fluid fraction
s	solid fraction
nf	nanofluid fraction



UUM
Universiti Utara Malaysia

List of Appendices

Appendix A Similarity Transformation	224
Appendix B Derivations of the Stability Analysis.....	238
Appendix C Runge-Kutta Fourth Order and Newton-Raphson Method	255
Appendix D Maple Program.....	259
Appendix E MATLAB Program for the Stability Analysis.....	263
Appendix F List of Publications	276



UUM
Universiti Utara Malaysia

CHAPTER ONE

INTRODUCTION

1.1 Introduction

This chapter contains an introduction of the nanofluid with the explanation of two well known nanofluid models and the base fluid. The boundary layer flows with the explanation of the velocity, thermal, and concentration boundary layers also given in this chapter. Dimensionless quantities, problem statement, research questions, objectives and scope, research methodology, significance of the present study are also described. The layout of the thesis is given in the last section of this chapter.

1.2 Nanofluid

Heat transfer is a major process in engineering and manufacturing of technological products where low thermal conductivities of common fluids keep fundamental limits. The common convectonal fluids such as ethylene glycol, engine oil, and water, have low thermal conductivities compared to solid's thermal conductivities. To increase the thermal conductivities of the convectonal fluids, small sized of the solid's particles can be employed. It has been proven by many researchers that micrometers or millimeters sized of the solid particles give significant heat transfer rate. The major issue was the settlements of the solid particles in the base fluid, which prevented many applications of the base fluids in the applications of heat transfer. After the discovery of carbon nanotubes by Oberlin, Endo, & Koyama (1970), nanotechnology developed rapidly and achieved much importance in the various fields of research (Oberline, Endo, & Koyama, 1976). Consequently, the concept of the mixing nanoparticles in a convectonal fluids in order to enhance the thermal conductivities was given by Choi and Eastman (1995). Such suspension of nanoparticles smaller than 1nm-100nm sized

REFERENCES

- Ahmad, A. (2012). *Flow and Heat Transfer Analysis for Arbitrary and Hyperbolic Stretching Surfaces* (Doctoral dissertation, COMSATS Institute of Information Technology Islamabad-Pakistan).
- Ahmadi, G. (1976). Self-similar solution of incompressible micropolar boundary layer flow over a semi-infinite plate. *International Journal of Engineering Science*, 14(7), 639-646.
- Aleng, N. L., Bachok, N., & Arifin, N. M. (2014). Boundary Layer Flow of a Nanofluid and Heat Transfer over an Exponentially Shrinking Sheet: Copper-Water. *transformation*, 1, 2.
- Alexander, J. S. (2017). *A Physical Introduction to Fluid Mechanics* (2nd ed.). Princeton University. (book).
- Ali, A. (2010). *Unsteady Micropolar Boundary Layer Flow and Convective Heat Transfer* (Doctoral dissertation). Universiti Teknologi Malaysia.
- Ali, M. E. (1995). On thermal boundary layer on a power-law stretched surface with suction or injection. *International Journal of Heat and Fluid Flow*, 16(4), 280-290.
- Ali, M. Y., & Hafez, M. G. (2012). A Case of Similarity Solutions for Unsteady Laminar Boundary Layer Flow in Curvilinear Surface. *ARPJ Journal of Engineering and Applied Science*, 7, 731-739.
- Al-Odat, M. Q., Damseh, R.A., and Al-Azab, T.A. (2006) Thermal boundary layer on an exponentially stretching continuous surface in the presence of magnetic field effect. *International Journal of Applied Mechanics and Engineering*, 11, 289 – 299.
- Alwawi, F. A., Alkawasbeh, H. T., Rashad, A. M., & Idris, R. (2020). MHD natural convection of Sodium Alginate Casson nanofluid over a solid sphere. *Results in Physics*, 16, 102818.
- Anwar, M. A. (2013). *Heat and mass transfer of magnetohydrodynamic boundary layer stagnation point flow of nanofluid over a stretching surface* (Doctoral dissertation). Universiti Teknologi Malaysia.
- Arqub, O. A., El-Ajou, A., Al-Zhour, Z., & Momani, S. (2014). Multiple solutions of nonlinear boundary value problems of fractional order: a new analytic iterative technique. *Entropy*, 16(1), 471-493.
- Ashraf, M., Kamal, M. A., & Syed, K. S. (2009). Numerical simulation of flow of a micropolar fluid between a porous disk and a non-porous disk. *Applied Mathematical Modelling*, 33(4), 1933-1943.

- Bachok, N., Ishak, A., & Pop, I. (2012). Unsteady boundary-layer flow and heat transfer of a nanofluid over a permeable stretching/shrinking sheet. *International Journal of Heat and Mass Transfer*, 55(7-8), 2102-2109.
- Batchelor, C. K., & Batchelor, G. K. (2000). *An introduction to fluid dynamics*. Cambridge university press.
- Bejan, A. (2013). *Convection heat transfer* (4th edition). John wiley & sons.
- Bergman, T. L., Incropera, F. P., DeWitt, D. P., & Lavine, A. S. (2011). *Fundamentals of heat and mass transfer*. John Wiley & Sons.
- Besthapu, P., & Bandari, S. (2015). Mixed convection MHD flow of a Casson nanofluid over a nonlinear permeable stretching sheet with viscous dissipation. *Journal of Applied Mathematics and Physics*, 3(12), 1580.
- Bhattacharyya, K., Mukhopadhyay, S., Layek, G. C., & Pop, I. (2012). Effects of thermal radiation on micropolar fluid flow and heat transfer over a porous shrinking sheet. *International Journal of Heat and Mass Transfer*, 55(11-12), 2945-2952.
- Bidin, B., & Nazar, R. (2009). Numerical solution of the boundary layer flow over an exponentially stretching sheet with thermal radiation. *European journal of scientific research*, 33(4), 710-717.
- Blasius, H. (1908). *Grenzschichten in Flüssigkeiten mit kleiner Reibung*. Druck von BG Teubner.
- Blazek, J. (2015). *Computational fluid dynamics: principles and applications*. Butterworth-Heinemann.
- Buongiorno, J. (2006). Convective transport in nanofluids. *J. Heat Transfer*, 128 (3), 240-250.
- Casson, N. (1959). *A flow equation for pigment-oil suspensions of the printing ink type*. Pergamon press.
- Cebeci, T. (2002). *Convective heat transfer*. 2. rev. ed. Germany.
- Chen, C. H. (1998). Laminar mixed convection adjacent to vertical, continuously stretching sheets. *Heat and Mass Transfer*, 33(5-6), 471-476.
- Chen, H., Xiao, T., & Shen, M. (2017). Nanofluid flow in a porous channel with suction and chemical reaction using Tiwari and Das's nanofluid model. *Heat Transfer—Asian Research*, 46(7), 1041-1052.
- Chhabra, R. P. (2010). Non-Newtonian fluids: an introduction. In *Rheology of complex fluids* (pp. 3-34). Springer, New York, NY.

- Choi, S. U. S., Zhang, Z. G., Keblinski, P. (2004,) Nanofluids, in Encyclopedia of Nanoscience and Nanotechnology, *American Scientific*, 6, 757–737.
- Choi, S. U. S., Zhang, Z. G., Yu, W., Lockwood, F. E., & Grulke, E. A. (2001). Anomalous thermal conductivity enhancement in nanotube suspensions. *Applied physics letters*, 79(14), 2252-2254.
- Choi, S. U., & Eastman, J. A. (1995). *Enhancing thermal conductivity of fluids with nanoparticles* (No. ANL/MSD/CP-84938; CONF-951135-29). Argonne National Lab., IL (United States).
- Chon, C. H., & Kihm, K. D. (2005). Thermal conductivity enhancement of nanofluids by Brownian motion. *Transactions-American Society of Mechanical Engineers Journal of Heat Transfer*, 127(8), 810.
- Crane, L. J. (1970). Flow past a stretching plate. *Zeitschrift für angewandte Mathematik und Physik ZAMP*, 21(4), 645-647.
- Das, K., & Duari, P. R. (2017). Micropolar nanofluid flow over an stretching sheet with chemical reaction. *International Journal of Applied and Computational Mathematics*, 3(4), 3229-3239.
- Das, S. K., Choi, S. U., Yu, W., & Pradeep, T. (2007). *Nanofluids: science and technology*. John Wiley & Sons.
- Ding, Y., Chen, H., Wang, L., Yang, C. Y., He, Y., Yang, W., ... & Huo, R. (2007). Heat transfer intensification using nanofluids. *KONA Powder and Particle Journal*, 25, 23-38.
- Ebaid, A., Al Mutairi, F., & Khaled, S. M. (2014). Effect of velocity slip boundary condition on the flow and heat transfer of Cu-water and TiO₂-water nanofluids in the presence of a magnetic field. *Advances in Mathematical Physics*, 2014.
- Elbashbeshy, E. M. A. (2001). Heat transfer over an exponentially stretching continuous surface with suction. *Archives of Mechanics*, 53(6), 643-651.
- Eringen, A. C. (1964). Simple microfluids. *International Journal of Engineering Science*, 2(2), 205-217.
- Eringen, A. C. (1966). Theory of micropolar fluids. *Journal of Mathematics and Mechanics*, 1-18.
- Fang, T. (2008). Boundary layer flow over a shrinking sheet with power-law velocity. *International Journal of Heat and Mass Transfer*, 51(25-26), 5838-5843.
- Favre-Marinet, M., & Tardu, S. (2013). *Convective heat transfer*. John Wiley & Sons.
- Fox, L. and Mayers, D.F. (1990) Numerical solution of ordinary differential equations for scientist and engineers, New York: Chapman and Hall.

- Gangaiah, T., Saidulu, N., & Venkata Lakshmi, A. (2019). The Influence of Thermal Radiation on Mixed Convection MHD Flow of a Casson Nanofluid over an Exponentially Stretching Sheet. *International Journal of Nanoscience and Nanotechnology*, 15(2), 83-98.
- Gelfgat, A. Y., & Bar-Yoseph, P. Z. (2004). Multiple solutions and stability of confined convective and swirling flows—a continuing challenge. *International Journal of Numerical Methods for Heat & Fluid Flow.*, 213 – 241.
- Ghosh, S., & Mukhopadhyay, S. (2019). Stability analysis for model-based study of nanofluid flow over an exponentially shrinking permeable sheet in presence of slip. *Neural Computing and Applications*, 1-11.
- Greenspan, D. (2006) Numerical solution of ordinary differential equations for classical, relativistic and nano system, Germany: Wiley-VCH Verlag.
- Hamid, M., Usman, M., Khan, Z. H., Ahmad, R., & Wang, W. (2019). Dual solutions and stability analysis of flow and heat transfer of Casson fluid over a stretching sheet. *Physics Letters A*, 383, 2400-2408.
- Haq, R., Nadeem, S., Khan, Z., & Okedayo, T. (2014). Convective heat transfer and MHD effects on Casson nanofluid flow over a shrinking sheet. *Open Physics*, 12(12), 862-871.
- Harris, S. D., Ingham, D. B., & Pop, I. (2009). Mixed convection boundary-layer flow near the stagnation point on a vertical surface in a porous medium: Brinkman model with slip. *Transport in Porous Media*, 77(2), 267-285.
- Hatami, M., & Ganji, D. D. (2014). Natural convection of sodium alginate (SA) non-Newtonian nanofluid flow between two vertical flat plates by analytical and numerical methods. *Case Studies in Thermal Engineering*, 2, 14-22.
- Hayat, T., Ashraf, M. B., Shehzad, S. A., & Alsaedi, A. (2015). Mixed Convection Flow of Casson Nanofluid over a Stretching Sheet with Convectively Heated Chemical Reaction and Heat Source/Sink. *Journal of Applied Fluid Mechanics*, 8(4).
- Hayat, T., Khan, M. I., Waqas, M., Alsaedi, A., & Khan, M. I. (2017). Radiative flow of micropolar nanofluid accounting thermophoresis and Brownian moment. *International Journal of Hydrogen Energy*, 42(26), 16821-16833.
- Hayat, T., Khan, M. I., Waqas, M., Alsaedi, A., & Khan, M. I. (2017). Radiative flow of micropolar nanofluid accounting thermophoresis and Brownian moment. *International Journal of Hydrogen Energy*, 42(26), 16821-16833.
- Hussanan, A., Khan, I., Gorji, M. R., & Khan, W. A. (2019). CNTs-Water-Based Nanofluid Over a Stretching Sheet. *BioNanoScience*, 9(1), 21-29.

- Imran, S. M. (2013). *Flow and Heat Transfer Over Stretching and Shrinking Surfaces* (Doctoral dissertation, COMSATS Institute of Information Technology Islamabad-Pakistan).
- Incropera, F. P., Lavine, A. S., Bergman, T. L., & DeWitt, D. P. (2007). *Fundamentals of heat and mass transfer*. Wiley.
- Ishak, A. (2014). Dual solutions in mixed convection boundary layer flow: A stability analysis. *Int. J. Math. Comput. Phys. Quantum Eng*, 8, 1131-1134.
- Jaluria, Y. and Torrance, K.E. (2003) *Computational Heat Transfer*, (2nd ed). New York: Taylor & Francis.
- Jang, S. P., & Choi, S. U. (2004). Role of Brownian motion in the enhanced thermal conductivity of nanofluids. *Applied physics letters*, 84(21), 4316-4318.
- Jat, R. N., & Chand, G. (2013). MHD flow and heat transfer over an exponentially stretching sheet with viscous dissipation and radiation effects. *Applied Mathematical Sciences*, 7(4), 167-180.
- Javed, T., Abbas, Z., Sajid, M., & Ali, N. (2011). Heat transfer analysis for a hydromagnetic viscous fluid over a non-linear shrinking sheet. *International Journal of Heat and Mass Transfer*, 54(9-10), 2034-2042.
- Jiji, L. M., & Jiji, L. M. (2006). *Heat convection*. Berlin: Springer.
- Jusoh, R., Nazar, R., & Pop, I. (2019). Magnetohydrodynamic boundary layer flow and heat transfer of nanofluids past a bidirectional exponential permeable stretching/shrinking sheet with viscous dissipation effect. *Journal of Heat Transfer*, 141(1).
- Kamal, F., Zaimi, K., Ishak, A., & Pop, I. (2018). Stability analysis on the stagnation-point flow and heat transfer over a permeable stretching/shrinking sheet with heat source effect. *International Journal of Numerical Methods for Heat & Fluid Flow*.
- Kamala, G., Gangadhar, K., Ramanamurthy, M. V., & Suresh, P. MHD Mixed Convection Flow of casson Nanofluid over a Non-Linear Permeable Stretching Sheet in The Presence of Heat Generation or Absorption.
- Kameswaran, P. K., Shaw, S., Sibanda, P. V. S. N., & Murthy, P. V. S. N. (2013). Homogeneous-heterogeneous reactions in a nanofluid flow due to a porous stretching sheet. *International Journal of Heat and Mass Transfer*, 57(2), 465-472.
- Kataria, H. R., & Mittal, A. S. (2017). Analysis of Casson nanofluid flow in presence of magnetic field and radiation. *Mathematics Today*, 33(1), 99-120.

- Khan, A., Khan, D., Khan, I., Ali, F., ul Karim, F., & Imran, M. (2018). MHD flow of Sodium Alginate-based Casson type nanofluid passing through a porous medium with Newtonian heating. *Scientific reports*, 8(1), 1-12.
- Khan, J. A., Mustafa, M., Hayat, T., Turkyilmazoglu, M., & Alsaedi, A. (2017). Numerical study of nanofluid flow and heat transfer over a rotating disk using Buongiorno's model. *International Journal of Numerical Methods for Heat & Fluid Flow*.
- Khan, M. S., Alam, M. M., & Ferdows, M. (2011). Finite difference solution of MHD radiative boundary layer flow of a nanofluid past a stretching sheet. In *Proceeding of the International Conference of Mechanical Engineering (ICME'11)*.
- Khan, S. K., & Sanjayanand, E. (2005). Viscoelastic boundary layer flow and heat transfer over an exponential stretching sheet. *International Journal of Heat and Mass Transfer*, 48(8), 1534-1542.
- Khan, W. A., & Pop, I. (2010). Boundary-layer flow of a nanofluid past a stretching sheet. *International journal of heat and mass transfer*, 53(11-12), 2477-2483.
- Khanafar, K., Vafai, K., & Lightstone, M. (2003). Buoyancy-driven heat transfer enhancement in a two-dimensional enclosure utilizing nanofluids. *International journal of heat and mass transfer*, 46(19), 3639-3653.
- Khashi'ie, N. S., Arifin, N. M., Pop, I., Nazar, R., Hafidzuddin, E. H., & Wahi, N. (2020). Non-axisymmetric Homann stagnation point flow and heat transfer past a stretching/shrinking sheet using hybrid nanofluid. *International Journal of Numerical Methods for Heat & Fluid Flow*.
- Khashi'ie, N. S., Md Arifin, N., Nazar, R., Hafidzuddin, E. H., Wahi, N., & Pop, I. (2019). Mixed Convective Flow and Heat Transfer of a Dual Stratified Micropolar Fluid Induced by a Permeable Stretching/Shrinking Sheet. *Entropy*, 21(12), 1162.
- Kim, S. H., Choi, S. R., & Kim, D. (2007). Thermal conductivity of metal-oxide nanofluids: particle size dependence and effect of laser irradiation. *Journal of Heat Transfer*, 129(3), 298-307
- Kümmerer, H. (1977). Similar laminar boundary layers in incompressible micropolar fluids. *Rheologica Acta*, 16(3), 261-265.
- Kuznetsov, A. V., & Nield, D. A. (2010). Natural convective boundary-layer flow of a nanofluid past a vertical plate. *International Journal of Thermal Sciences*, 49(2), 243-247.
- Kuznetsov, A. V., & Nield, D. A. (2013). The Cheng–Minkowycz problem for natural convective boundary layer flow in a porous medium saturated by a nanofluid: a revised model. *International Journal of Heat and Mass Transfer*, 65, 682-685.

- Kuznetsov, A. V., & Nield, D. A. (2014). Natural convective boundary-layer flow of a nanofluid past a vertical plate: A revised model. *International journal of thermal sciences*, 77, 126-129.
- Lienhard IV. J. H., & Lienhard V. J. H. (2019). *A heat transfer book* (5th ed.). Courier Dover Publications, New York.
- Lok, Y. Y. (2008). *Mathematical modelling of a micropolar fluid boundary layer near a stagnation-point* (Doctoral dissertation). Universiti Teknologi Malalaysia.
- Lund, L. A., Omar, Z., Dero, S., & Khan, I. (2020). Linear stability analysis of MHD flow of micropolar fluid with thermal radiation and convective boundary condition: Exact solution. *Heat Transfer—Asian Research*, 49(1), 461-476.
- Lund, L. A., Omar, Z., Khan, I., & Dero, S. (2019). Multiple solutions of Cu-C 6 H 9 NaO 7 and Ag-C 6 H 9 NaO 7 nanofluids flow over nonlinear shrinking surface. *Journal of Central South University*, 26(5), 1283-1293.
- Lund, L. A., Omar, Z., Khan, I., Kadry, S., Rho, S., Mari, I. A., & Nisar, K. S. (2019). Effect of Viscous Dissipation in Heat Transfer of MHD Flow of Micropolar Fluid Partial Slip Conditions: Dual Solutions and Stability Analysis. *Energies*, 12(24), 4617.
- Lund, L. A., Omar, Z., Khan, I., Raza, J., Bakouri, M., & Tlili, I. (2019). Stability analysis of Darcy-Forchheimer flow of Casson type nanofluid over an exponential sheet: Investigation of critical points. *Symmetry*, 11(3), 412.
- Mabood, F., Khan, W. A., & Ismail, A. M. (2017). MHD flow over exponential radiating stretching sheet using homotopy analysis method. *Journal of King Saud University-Engineering Sciences*, 29(1), 68-74.
- Magyari, E., & Keller, B. (1999). Heat and mass transfer in the boundary layers on an exponentially stretching continuous surface. *Journal of Physics D: Applied Physics*, 32(5), 577.
- Mahapatra, T. R., & Nandy, S. K. (2011). Stability analysis of dual solutions in stagnation-point flow and heat transfer over a Power-law shrinking surface. *International Journal of Nonlinear Science*, 12(1), 86-94.
- Mahmoud, M. A. (2007). Thermal radiation effects on MHD flow of a micropolar fluid over a stretching surface with variable thermal conductivity. *Physica A: Statistical Mechanics and its Applications*, 375(2), 401-410.
- Maïga, S. E. B., Nguyen, C. T., Galanis, N., & Roy, G. (2004). Heat transfer behaviors of nanofluids in a uniformly heated tube. *Superlattices and Microstructures*, 35(3-6), 543-557.
- Makinde, O. D., & Aziz, A. (2011). Boundary layer flow of a nanofluid past a stretching sheet with a convective boundary condition. *International Journal of Thermal Sciences*, 50(7), 1326-1332.

- Malga, B. S., & Kishan, N. (2013). Viscous Dissipation Effects on Unsteady free Convection and Mass Transfer Flow of Micropolar Fluid Embedded in a Porous Media with Chemical Reaction. *Elixir Appl. Math*, 63, 18569-18578.
- Malik, M. Y., Naseer, M., Nadeem, S., & Rehman, A. (2014). The boundary layer flow of Casson nanofluid over a vertical exponentially stretching cylinder. *Applied Nanoscience*, 4(7), 869-873.
- Mansur, S., & Ishak, A. (2016). Unsteady boundary layer flow of a nanofluid over a stretching/shrinking sheet with a convective boundary condition. *Journal of the Egyptian Mathematical Society*, 24(4), 650-655.
- Maripala, S., & Kishan, N. (2017). Chemical Reaction Effects on MHD Nanofluid Flow of a Convection Slip in a Saturated Porous Media Over a Radiating Stretching Sheet with Heat Source/Sink. *Asian Research Journal of Mathematics*, 1-15.
- Meade, D. B., Haran, B. S., & White, R. E. (1996). The shooting technique for the solution of two-point boundary value problems. *Maple Technical Newsletter*, 3(1), 1-8.
- Merkin, J. H. (1980). Mixed convection boundary layer flow on a vertical surface in a saturated porous medium. *Journal of Engineering Mathematics*, 14(4), 301-313.
- Merkin, J. H. (1986). On dual solutions occurring in mixed convection in a porous medium. *Journal of engineering Mathematics*, 20(2), 171-179.
- Miklavčič, M., & Wang, C. (2006). Viscous flow due to a shrinking sheet. *Quarterly of Applied Mathematics*, 64(2), 283-290.
- Mondal, M., Biswas, R., Shanchia, K., Hasan, M., & Ahmmed, S. F. (2019). Numerical Investigation with Stability Convergence Analysis of Chemically Hydromagnetic Casson Nanofluid Flow in the Effects of Thermophoresis and Brownian Motion. *Journal homepage: <http://iieta.org/Journals/LJHT>*, 37(1), 59-70.
- Mondal, M., Biswas, R., Shanchia, K., Hasan, M., & Ahmmed, S. F. (2019). Numerical investigation with stability convergence analysis of chemically hydromagnetic Casson nanofluid flow in the effects of thermophoresis and Brownian motion. *Journal homepage: <http://iieta.org/Journals/LJHT>*, 37(1), 59-70.
- Mustafa, I., Abbas, Z., Arif, A., Javed, T., & Ghaffari, A. (2020). Stability analysis for multiple solutions of boundary layer flow towards a shrinking sheet: Analytical solution by using least square method. *Physica A: Statistical Mechanics and its Applications*, 540, 123028.
- Mutuku-Njane, W. N. (2014). *Analysis of hydromagnetic boundary layer flow and heat transfer of nanofluids* (Doctoral dissertation, Cape Peninsula University of Technology).

- Nadeem, S., & Lee, C. (2012). Boundary layer flow of nanofluid over an exponentially stretching surface. *Nanoscale research letters*, 7(1), 94.
- Nadeem, S., Haq, R. U., & Akbar, N. S. (2013). MHD three-dimensional boundary layer flow of Casson nanofluid past a linearly stretching sheet with convective boundary condition. *IEEE Transactions on Nanotechnology*, 13(1), 109-115.
- Nadeem, S., Haq, R. U., & Khan, Z. H. (2014). Heat transfer analysis of water-based nanofluid over an exponentially stretching sheet. *Alexandria Engineering Journal*, 53(1), 219-224.
- Nakamura, M., & Sawada, T. (1988). Numerical study on the flow of a non-Newtonian fluid through an axisymmetric stenosis.
- Nazar, R., & Pop, I. (2006). Mixed Convection Boundary Layer Flow Over A Vertical Permeable Plate In A Porous Medium: Opposing Flow Case. *Journal of Technology*, 45 (1), 1-14.
- Nield, D. A., & Bejan, A. (2006). *Convection in porous media* (Vol. 3). New York: springer.
- Noghrehabadi, A., Ghalambaz, M., Ghalambaz, M., & Ghanbarzadeh, A. (2012). Comparing thermal enhancement of Ag-water and SiO₂-water nanofluids over an isothermal stretching sheet with suction or injection. *Journal of Computational & Applied Research in Mechanical Engineering (JCARME)*, 2(1), 37-49.
- Oberlin, A., Endo, M., & Koyama, T. (1976). High resolution electron microscope observations of graphitized carbon fibers. *Carbon*, 14(2), 133-135.
- Othman, N. A., Yacob, N. A., Bachok, N., Ishak, A., & Pop, I. (2017). Mixed convection boundary-layer stagnation point flow past a vertical stretching/shrinking surface in a nanofluid. *Applied Thermal Engineering*, 115, 1412-1417.
- Peddieson, J. (1970) Boundary-layer theory for a micropolar fluid. *Recent Adv. Eng.Sci.5*, 405–426.
- Pop, I., & Ingham, D. B. (2001). *Convective heat transfer: mathematical and computational modelling of viscous fluids and porous media*. Elsevier.
- Prasad, A. K., & Koseff, J. R. (1996). Combined forced and natural convection heat transfer in a deep lid-driven cavity flow. *International Journal of Heat and Fluid Flow*, 17(5), 460-467.
- Rahman, M. M., Roşca, A. V., & Pop, I. (2014). Boundary layer flow of a nanofluid past a permeable exponentially shrinking/stretching surface with second order slip using Buongiorno's model. *International Journal of Heat and Mass Transfer*, 77, 1133-1143.

- Rajpuit, R. K. (2007). *A textbook of fluid mechanics and hydraulic machines: (in S. I unit)*. New Dehli. India: S. Chand.
- RamReddy, C., & Muralikrishna, P. (2017). Effects of First and Second Order Velocity Slips on Melting Stretching Surface in a Thermally Stratified Nanofluid: Tiwari and Das' Model. *Journal of Nanofluids*, 6(1), 155-163.
- Ramzan, M., Chung, J. D., & Ullah, N. (2017). Partial slip effect in the flow of MHD micropolar nanofluid flow due to a rotating disk—A numerical approach. *Results in physics*, 7, 3557-3566.
- Rana, P., Shukla, N., Gupta, Y., & Pop, I. (2019). Homotopy analysis method for predicting multiple solutions in the channel flow with stability analysis. *Communications in Nonlinear Science and Numerical Simulation*, 66, 183-193
- Rao, J. A., Prasad, R. S., & Ramya, D. (2016). MHD Boundary Layer Flow and Heat Transfer of Nanofluids over a Nonlinear Stretching Sheet in a Porous Medium. *IOSR Journal of Mathematics*, 12(2), 1-10.
- Raza, J. (2018). Similarity Solutions of Boundary Layer Flows in A Channel Filled By Non-Newtonian Fluids (Doctoral dissertation). Universiti Utara Malaysia.
- Raza, J., Rohni, A. M., & Omar, Z. (2016). Rheology of micropolar fluid in a channel with changing walls: Investigation of multiple solutions. *Journal of Molecular Liquids*, 223, 890-902.
- Roberts S.M. and Shipman, J.S. (1972) Two-point boundary value problems: Shooting Methods. New York: American Elsevier
- Rohni, A. M. (2013). *Multiple Similarity Solutions of Steady and Unsteady Convection Boundary Layer Flows in Viscous Fluids and Nanofluids* (Doctoral dissertation). Universiti Sains Malaysia.
- Rohni, A. M., Ahmad, S., Ismail, A. I. M., & Pop, I. (2013). Boundary layer flow and heat transfer over an exponentially shrinking vertical sheet with suction. *International journal of thermal sciences*, 64, 264-272.
- Rohni, A. M., Ahmad, S., Ismail, A. I. M., & Pop, I. (2013). Flow and heat transfer over an unsteady shrinking sheet with suction in a nanofluid using Buongiorno's model. *International Communications in Heat and Mass Transfer*, 43, 75-80.
- Roşca, A. V., & Pop, I. (2014). Flow and heat transfer of Powell–Eyring fluid over a shrinking surface in a parallel free stream. *International Journal of Heat and Mass Transfer*, 71, 321-327.
- Roy, G., Nguyen, C. T., & Lajoie, P. R. (2004). Numerical investigation of laminar flow and heat transfer in a radial flow cooling system with the use of nanofluids. *Superlattices and Microstructures*, 35(3-6), 497-511.

- Sajid, M., & Hayat, T. (2008). Influence of thermal radiation on the boundary layer flow due to an exponentially stretching sheet. *International Communications in Heat and Mass Transfer*, 35(3), 347-356.
- Sakiadis, B. C. (1961). Boundary layer behavior on continuous solid surfaces: I. Boundary layer equations for two-dimensional and axisymmetric flow. *AIChE Journal*, 7(1), 26-28.
- Sanjayanand, E., & Khan, S. K. (2006). On heat and mass transfer in a viscoelastic boundary layer flow over an exponentially stretching sheet. *International Journal of Thermal Sciences*, 45(8), 819-828.
- Saqib, M., Khan, I., & Shafie, S. (2019). Shape Effect in Magnetohydrodynamic Free Convection Flow of Sodium Alginate-Ferrimagnetic Nanofluid. *Journal of Thermal Science and Engineering Applications*, 11(4).
- Sheremet, M. A., Grosan, T., & Pop, I. (2015). Free convection in a square cavity filled with a porous medium saturated by nanofluid using Tiwari and Das' nanofluid model. *Transport in Porous Media*, 106(3), 595-610.
- Tiwari, R. K., & Das, M. K. (2007). Heat transfer augmentation in a two-sided lid-driven differentially heated square cavity utilizing nanofluids. *International Journal of heat and Mass transfer*, 50(9-10), 2002-2018.
- Tsou, F. K., Sparrow, E. M., & Goldstein, R. J. (1967). Flow and heat transfer in the boundary layer on a continuous moving surface. *International Journal of Heat and Mass Transfer*, 10(2), 219-235.
- Usama, Nadeem, S., & Khan, A. U. (2019). Stability analysis of Cu-H₂O nanofluid over a curved stretching-shrinking sheet: existence of dual solutions. *Canadian Journal of Physics*, 97(8), 911-922.
- Vajravelu, K., Prasad, K. V., & Ng, C. O. (2013). The effect of variable viscosity on the flow and heat transfer of a viscous Ag-water and Cu-water nanofluids. *Journal of Hydrodynamics*, 25(1), 1-9.
- Vajravelu, K., Prasad, K. V., Lee, J., Lee, C., Pop, I., & Van Gorder, R. A. (2011). Convective heat transfer in the flow of viscous Ag-water and Cu-water nanofluids over a stretching surface. *International Journal of Thermal Sciences*, 50(5), 843-851.
- Van Vliet, M. T., Wiberg, D., Leduc, S., & Riahi, K. (2016). Power-generation system vulnerability and adaptation to changes in climate and water resources. *Nature Climate Change*, 6(4), 375-380.
- Waini, I., Ishak, A., & Pop, I. (2020). MHD flow and heat transfer of a hybrid nanofluid past a permeable stretching/shrinking wedge. *Applied Mathematics and Mechanics*, 1-14.

- Waini, I., Ishak, A., & Pop, I. (2020a). Transpiration effects on hybrid nanofluid flow and heat transfer over a stretching/shrinking sheet with uniform shear flow. *Alexandria Engineering Journal*, 59(1), 91-99.
- Wang, C. Y. (2011). Review of similarity stretching exact solutions of the Navier-Stokes equations. *European Journal of Mechanics-B/Fluids*, 30(5), 475-479.
- Wang, X. Q., & Mujumdar, A. S. (2007). Heat transfer characteristics of nanofluids: a review. *International journal of thermal sciences*, 46(1), 1-19.
- Wang, X., & Wang, J. (2017). Numerical simulation of natural convection in a triangle cavity filled with nanofluids using Tiwari and Das' model: Effects of heat flux. *Heat Transfer—Asian Research*, 46(7), 761-777.
- Weidman, P. D., Davis, A. M. J., & Kubitschek, D. G. (2008). Crocco variable formulation for uniform shear flow over a stretching surface with transpiration: multiple solutions and stability. *Zeitschrift für angewandte Mathematik und Physik*, 59(2), 313-332.
- Weidman, P. D., Kubitschek, D. G., & Davis, A. M. J. (2006). The effect of transpiration on self-similar boundary layer flow over moving surfaces. *International journal of engineering science*, 44(11-12), 730-737.
- Wilks, G., & Bramley, J. S. (1981). Dual solutions in mixed convection. *Proceedings of the Royal Society of Edinburgh Section A: Mathematics*, 87(3-4), 349-358.
- Xuan, Y., & Roetzel, W. (2000). Conceptions for heat transfer correlation of nanofluids. *International Journal of heat and Mass transfer*, 43(19), 3701-3707.
- Yacob, N. A., Ishak, A., Pop, I., & Vajravelu, K. (2011). Boundary layer flow past a stretching/shrinking surface beneath an external uniform shear flow with a convective surface boundary condition in a nanofluid. *Nanoscale research letters*, 6(1), 314.
- Yao, L. S. (2009). Multiple solutions in fluid dynamics. *Nonlinear Analysis: Modelling and Control*, 14 (2), 263 – 279.
- You, S. M., Kim, J. H., & Kim, K. H. (2003). Effect of nanoparticles on critical heat flux of water in pool boiling heat transfer. *Applied physics letters*, 83(16), 3374-3376.
- Zaimi, K., Ishak, A., & Pop, I. (2014). Flow past a permeable stretching/shrinking sheet in a nanofluid using two-phase model. *Plos one*, 9(11).

APPENDIX A

SIMILARITY TRANSFORMATION

BOUNDARY LAYER FLOW OF CASSON NANOFUID OVER A PERMEABLE EXPONENTIALLY SHRINKING/STRETCHING SHEET: TIWARI AND DAS's MODEL

Governing equations

The governing equations of continuity, momentum and heat transfer are

$$\frac{\partial u}{\partial x} + \frac{\partial v}{\partial y} = 0 \quad (8.1)$$

$$u \frac{\partial u}{\partial x} + v \frac{\partial u}{\partial y} = \frac{\mu_{nf}}{\rho_{nf}} \left[\left(1 + \frac{1}{\beta} \right) \frac{\partial^2 u}{\partial y^2} + g(\rho\beta)_{nf}(T - T_\infty) \right] \quad (8.2)$$

$$u \frac{\partial T}{\partial x} + v \frac{\partial T}{\partial y} = \frac{1}{(\rho C_p)_{nf}} \left[k_{nf} \left(1 + \frac{16T_\infty^3 \sigma^*}{3k_{nf} k^*_f} \right) \frac{\partial^2 T}{\partial y^2} + Q(T - T_\infty) \right] \quad (8.3)$$

The boundary conditions of these equations are given as

$$v = v_w; u = \lambda u_w(x) + A \frac{\partial u}{\partial y}; T = T_w + D \frac{\partial T}{\partial y}; \quad \text{at } y = 0$$

$$u \rightarrow 0; T \rightarrow T_\infty; \quad \text{as } y \rightarrow \infty \quad (8.4)$$

For the similarity solutions, the following similarity transformations are used (Rohni, 2013).

$$\psi = \sqrt{2\theta l U_w} e^{x/2l} f(\eta); \theta(\eta) = \frac{T - T_\infty}{T_w - T_\infty}; \eta = y \sqrt{\frac{U_w}{2\theta l}} e^{x/2l} \quad (6.5)$$

where ψ is the stream function that is defined in the classical form as

$$u = \frac{\partial \psi}{\partial y}, v = -\frac{\partial \psi}{\partial x}$$

Thus we have

$$u = \frac{\partial \psi}{\partial y} = \frac{\partial(\sqrt{2a\vartheta_f L} e^{\frac{x}{2L}} f(\eta))}{\partial y}$$

$$u = \sqrt{2a\vartheta_f L} e^{\frac{x}{2L}} f'(\eta) \frac{\partial \eta}{\partial y}$$

$$u = \sqrt{2a\vartheta_f L} e^{\frac{x}{2L}} f'(\eta) \frac{\partial \left(y \sqrt{\frac{a}{2L\vartheta_f}} e^{\frac{x}{2L}} \right)}{\partial y}$$

$$u = \sqrt{2a\vartheta_f L} \frac{a}{2L\vartheta_f} e^{\frac{x}{2L}} f'(\eta)$$

$$u = a e^{\frac{x}{2L}} f'(\eta)$$

(A.1)

And

$$v = -\frac{\partial \psi}{\partial x} = -\sqrt{2a\vartheta_f L} \frac{\partial}{\partial x} \left(e^{\frac{x}{2L}} f(\eta) \right)$$

$$v = -\sqrt{2a\vartheta_f L} \left(\frac{1}{2L} e^{\frac{x}{2L}} f(\eta) + e^{\frac{x}{2L}} f'(\eta) \frac{\partial \eta}{\partial x} \right)$$

$$v = -\sqrt{2a\vartheta_f L} \left(\frac{1}{2L} e^{\frac{x}{2L}} f(\eta) + e^{\frac{x}{2L}} f'(\eta) \frac{\partial \left(y \sqrt{\frac{a}{2L\vartheta_f}} e^{\frac{x}{2L}} \right)}{\partial x} \right)$$

$$v = -\sqrt{2a\vartheta_f L} \left(\frac{1}{2L} e^{\frac{x}{2L}} f(\eta) + \frac{1}{2L} e^{\frac{x}{2L}} \eta \cdot f'(\eta) \right)$$

$$v = -\frac{1}{2L} \sqrt{2a\vartheta_f L} e^{\frac{x}{2L}} (f(\eta) + \eta \cdot f'(\eta))$$

$$v = -\sqrt{\frac{2a\vartheta_f L}{4L^2}} e^{\frac{x}{2L}} (f(\eta) + \eta \cdot f'(\eta))$$

$$v = -\sqrt{\frac{a\vartheta_f}{2L}} e^{\frac{x}{2L}} (f(\eta) + \eta \cdot f'(\eta)) \quad (A.2)$$

To solve the continuity equation (A.1), $\frac{\partial u}{\partial x}$ and $\frac{\partial v}{\partial y}$ will be obtained

$$\frac{\partial u}{\partial x} = a \frac{\partial}{\partial x} \left[e^{\frac{x}{L}} f'(\eta) \right]$$

$$\frac{\partial u}{\partial x} = a \left[\frac{1}{L} e^{\frac{x}{L}} f'(\eta) + e^{\frac{x}{L}} f''(\eta) \frac{\partial \eta}{\partial x} \right]$$

$$\frac{\partial u}{\partial x} = a \left[\frac{1}{L} e^{\frac{x}{L}} f'(\eta) + e^{\frac{x}{L}} f''(\eta) \frac{\partial}{\partial x} \left(y \sqrt{\frac{a}{2L\vartheta_f}} e^{\frac{x}{2L}} \right) \right]$$

$$\frac{\partial u}{\partial x} = a \left[\frac{1}{L} e^{\frac{x}{L}} f'(\eta) + \frac{1}{2L} e^{\frac{x}{L}} \eta f''(\eta) \right]$$

$$\frac{\partial u}{\partial x} = \frac{a}{2L} e^{\frac{x}{L}} [2f'(\eta) + \eta f''(\eta)] \quad (A.3)$$

$$\frac{\partial v}{\partial y} = \frac{\partial}{\partial y} \left(-\sqrt{\frac{a\vartheta_f}{2L}} e^{\frac{x}{2L}} (f(\eta) + \eta \cdot f'(\eta)) \right)$$

$$\frac{\partial v}{\partial y} = -\sqrt{\frac{a\vartheta_f}{2L}} e^{\frac{x}{2L}} \left[f'(\eta) \frac{\partial \eta}{\partial y} + \frac{\partial \eta}{\partial y} f'(\eta) + \eta \cdot f''(\eta) \frac{\partial \eta}{\partial y} \right]$$

$$\frac{\partial v}{\partial y} = -\sqrt{\frac{a\vartheta_f}{2L}} e^{\frac{x}{2L}} \frac{\partial \eta}{\partial y} [f'(\eta) + f'(\eta) + \eta \cdot f''(\eta)]$$

$$\frac{\partial v}{\partial y} = -\sqrt{\frac{a\theta_f}{2L}} e^{\frac{x}{2L}} \frac{\partial}{\partial y} \left(y \sqrt{\frac{a}{2L\theta_f}} e^{\frac{x}{2L}} \right) [2f'(\eta) + \eta \cdot f''(\eta)]$$

$$\frac{\partial v}{\partial y} = -\frac{a}{2L} e^{\frac{x}{L}} [2f'(\eta) + \eta \cdot f''(\eta)] \quad (A.4)$$

By substituting equations (A.3) and (A.4) into (A.1), we have

$$\frac{\partial u}{\partial x} + \frac{\partial v}{\partial y} = \frac{a}{2L} e^{\frac{x}{L}} [2f'(\eta) + \eta f''(\eta)] + \left(-\frac{a}{2L} e^{\frac{x}{L}} [2f'(\eta) + \eta \cdot f''(\eta)] \right)$$

$$\frac{\partial u}{\partial x} + \frac{\partial v}{\partial y} = \frac{a}{2L} e^{\frac{x}{L}} [2f'(\eta) + \eta f''(\eta) - 2f'(\eta) - \eta \cdot f''(\eta)]$$

$$\frac{\partial u}{\partial x} + \frac{\partial v}{\partial y} = 0$$

The continuity equation is satisfied.

Moreover, to get the similarity solution of the momentum equation (7.2) $\frac{\partial u}{\partial y}$, $\frac{\partial^2 u}{\partial y^2}$ and

$g(\rho\beta)_{nf}(T - T_\infty)$ are needed to be obtained

$$\frac{\partial u}{\partial y} = a e^{\frac{x}{L}} \frac{\partial}{\partial y} (f'(\eta))$$

$$\frac{\partial u}{\partial y} = a e^{\frac{x}{L}} \left[f''(\eta) \frac{\partial \eta}{\partial y} \right]$$

$$\frac{\partial u}{\partial y} = a e^{\frac{x}{L}} \left[f''(\eta) \frac{\partial}{\partial y} \left(y \sqrt{\frac{a}{2L\theta_f}} e^{\frac{x}{2L}} \right) \right]$$

$$\frac{\partial u}{\partial y} = a \sqrt{\frac{a}{2L\theta_f}} e^{\frac{3x}{2L}} [f''(\eta)]$$

$$\frac{\partial u}{\partial y} = a \sqrt{\frac{a}{2L\theta_f}} e^{\frac{3x}{2L}} f''(\eta) \quad (A.5)$$

$$\frac{\partial^2 u}{\partial y^2} = a \sqrt{\frac{a}{2L\theta_f}} e^{\frac{3x}{2L}} \frac{\partial}{\partial y} [f''(\eta)]$$

$$\frac{\partial^2 u}{\partial y^2} = a \sqrt{\frac{a}{2L\theta_f}} e^{\frac{3x}{2L}} \left[f'''(\eta) \frac{\partial}{\partial y} \left(y \sqrt{\frac{a}{2L\theta_f}} e^{\frac{x}{2L}} \right) \right]$$

$$\frac{\partial^2 u}{\partial y^2} = \frac{a^2}{2L\theta_f} e^{\frac{2x}{L}} f'''(\eta) \quad (A.6)$$

$$\theta(\eta) = \frac{(T - T_\infty)}{(T_w - T_\infty)}$$

$$(T_w - T_\infty)\theta(\eta) = (T - T_\infty)$$

$$T = T_\infty + (T_w - T_\infty)\theta(\eta)$$

Then

$$T = T_\infty + T_0 e^{\frac{2x}{L}} \theta(\eta)$$

$$T - T_\infty = T_0 e^{\frac{2x}{L}} \theta(\eta)$$

$$g(\rho\beta)_{nf}(T - T_\infty) = g(\rho\beta)_{nf} T_0 e^{\frac{2x}{L}} \theta(\eta) \quad (A.7)$$

By substituting (A.1) – (A.7) in (8.2), it is obtained

$$\begin{aligned}
& a e^{\frac{x}{L}} f'(\eta) * \frac{a}{2L} e^{\frac{x}{L}} [2f'(\eta) + \eta f''(\eta)] - \sqrt{\frac{a\vartheta}{2L}} e^{\frac{x}{2L}} [f(\eta) + \eta f'(\eta)] \\
& * a \sqrt{\frac{a}{2L\vartheta_f}} e^{\frac{3x}{2L}} f''(\eta) \\
& = \frac{1}{\rho_{nf}} \left[\mu_{nf} \left(1 + \frac{1}{\beta}\right) \frac{a^2}{2L\vartheta_f} e^{\frac{2x}{L}} f'''(\eta) + g(\rho\beta)_{nf} T_0 e^{\frac{2x}{L}} \theta(\eta) \right]
\end{aligned}$$

$$\begin{aligned}
& \frac{a^2}{2L} e^{\frac{2x}{L}} f'(\eta) [2f'(\eta) + \eta f''(\eta)] - \frac{a^2}{2L} e^{\frac{2x}{L}} [f(\eta) + \eta f'(\eta)] f''(\eta) = \frac{a^2}{2L} e^{\frac{2x}{L}} \left[\frac{\mu_{nf}}{\rho_{nf}\vartheta_f} \left(1 + \frac{1}{\beta}\right) f'''(\eta) + \frac{1}{\rho_{nf}} \frac{2Lg(\rho\beta)_{nf}T_0}{a^2} \theta(\eta) \right]
\end{aligned}$$

$$\begin{aligned}
& \frac{a^2}{2L} e^{\frac{2x}{L}} \left[2(f'(\eta))^2 + \eta f'(\eta) f''(\eta) - f(\eta) f''(\eta) - \eta f'(\eta) f''(\eta) \right] \\
& = \frac{a^2}{2L} e^{\frac{2x}{L}} \left[\frac{\mu_{nf}}{\rho_{nf}\vartheta_f} \left(1 + \frac{1}{\beta}\right) f'''(\eta) + \frac{1}{\rho_{nf}} \frac{2Lg(\rho\beta)_{nf}T_0}{a^2} \theta(\eta) \right]
\end{aligned}$$

This implies that

$$\begin{aligned}
& \left[2(f'(\eta))^2 + \eta f'(\eta) f''(\eta) - f(\eta) f''(\eta) - \eta f'(\eta) f''(\eta) \right] = \left[\frac{\mu_{nf}}{\rho_{nf}\vartheta_f} \left(1 + \frac{1}{\beta}\right) f'''(\eta) + \frac{1}{\rho_{nf}} \frac{2Lg(\rho\beta)_{nf}T_0}{a^2} \theta(\eta) \right]
\end{aligned}$$

Simplifying it is obtained

$$2(f'(\eta))^2 - f(\eta) f''(\eta) = \frac{\mu_{nf}}{\rho_{nf}\vartheta_f} \left(1 + \frac{1}{\beta}\right) f'''(\eta) + \frac{1}{\rho_{nf}} \frac{2Lg(\rho\beta)_{nf}T_0}{a^2} \theta(\eta) \quad (A.8)$$

The thermo physical properties μ_{nf} , ρ_{nf} and $(\rho\beta)_{nf}$ are defined as

$$\mu_{nf} = \frac{\mu_f}{(1-\phi)^{2.5}} \quad (A.9)$$

$$\rho_{nf} = (1 - \phi)\rho_f + \phi\rho_s = \rho_f \left((1 - \phi) + \phi \left(\frac{\rho_s}{\rho_f} \right) \right) \quad (A.10)$$

$$(\rho\beta)_{nf} = (1 - \phi)(\rho\beta)_f + \phi(\rho\beta)_s = (\rho\beta)_f \left((1 - \phi) + \phi \frac{(\rho\beta)_s}{(\rho\beta)_f} \right) \quad (A.11)$$

By substituting (A.9), (A.10) and (A.11) in (A.8) we get

$$2(f'(\eta))^2 - f(\eta)f''(\eta) = \frac{1}{\rho_f \left((1 - \phi) + \phi \left(\frac{\rho_s}{\rho_f} \right) \right) \vartheta_f} \frac{\mu_f}{(1 - \phi)^{2.5}} \left(1 + \frac{1}{\beta} \right) f'''(\eta) +$$

$$\frac{(\rho\beta)_f \left((1 - \phi) + \phi \frac{(\rho\beta)_s}{(\rho\beta)_f} \right) 2gL T_0}{\rho_f \left((1 - \phi) + \phi \left(\frac{\rho_s}{\rho_f} \right) \right) a^2} \theta(\eta)$$

$$2(f'(\eta))^2 - f(\eta)f''(\eta) = \frac{1}{\left((1 - \phi) + \phi \left(\frac{\rho_s}{\rho_f} \right) \right)} \left[\frac{\mu_f}{\rho_f \vartheta_f} \frac{1}{(1 - \phi)^{2.5}} \left(1 + \frac{1}{\beta} \right) f'''(\eta) + \left((1 - \phi) + \phi \frac{(\rho\beta)_s}{(\rho\beta)_f} \right) \frac{2gL\rho_f\beta_f T_0}{\rho_f a^2} \theta(\eta) \right]$$

Re-arranging we get

$$2(f'(\eta))^2 - f(\eta)f''(\eta) = \frac{1}{\left((1 - \phi) + \phi \left(\frac{\rho_s}{\rho_f} \right) \right)} \left[\frac{1}{(1 - \phi)^{2.5}} \left(1 + \frac{1}{\beta} \right) f'''(\eta) + 2\zeta \left((1 - \phi) + \phi \frac{(\rho\beta)_s}{(\rho\beta)_f} \right) \theta(\eta) \right] \quad \text{where } \vartheta_f = \frac{\mu_f}{\rho_f}, \zeta = \frac{L^3 g \beta_f T_0}{\vartheta_f^2} \left/ \left(\frac{LU_w}{\vartheta_f} \right)^2 = \frac{Gr}{Re_x^2} \right.$$

After simplification finally it is obtained

$$\begin{aligned}
& \left(1 + \frac{1}{\beta}\right) f''''(\eta) \\
& + (1 - \phi)^{2.5} \left[\left((1 - \phi) + \phi \left(\frac{\rho_s}{\rho_f} \right) \right) (f(\eta) f''(\eta) - 2(f'(\eta))^2) \right. \\
& \left. + 2\zeta \left((1 - \phi) + \phi \frac{(\rho\beta)_s}{(\rho\beta)_f} \right) \theta(\eta) \right] = 0
\end{aligned}$$

To obtain similarity for energy equations (8.3), $\frac{\partial T}{\partial x}$, $\frac{\partial T}{\partial y}$ and $\frac{\partial^2 T}{\partial y^2}$ are required

$$\frac{\partial T}{\partial x} = \frac{\partial}{\partial x} \left(T_\infty + T_0 e^{\frac{2x}{L}} \theta(\eta) \right)$$

$$\frac{\partial T}{\partial x} = 0 + T_0 \frac{\partial}{\partial x} \left(e^{\frac{2x}{L}} \theta(\eta) \right)$$

$$\frac{\partial T}{\partial x} = T_0 \left(e^{\frac{2x}{L}} \theta(\eta) \frac{2}{L} + e^{\frac{2x}{L}} \theta'(\eta) \frac{\partial \eta}{\partial x} \right)$$

$$\frac{\partial T}{\partial x} = T_0 \left(e^{\frac{2x}{L}} \theta(\eta) \frac{2}{L} + e^{\frac{2x}{L}} \eta \cdot \theta'(\eta) \frac{1}{2L} \right)$$

$$\frac{\partial T}{\partial x} = \frac{T_0}{2L} e^{\frac{2x}{L}} (4\theta(\eta) + \eta \cdot \theta'(\eta))$$

(A.12)

$$\frac{\partial T}{\partial y} = \frac{\partial}{\partial y} \left(T_\infty + T_0 e^{\frac{2x}{L}} \theta(\eta) \right)$$

$$\frac{\partial T}{\partial y} = 0 + T_0 e^{\frac{2x}{L}} \frac{\partial \theta(\eta)}{\partial y}$$

$$\frac{\partial T}{\partial y} = T_0 e^{\frac{2x}{L}} \theta'(\eta) \frac{\partial \eta}{\partial y}$$

$$\frac{\partial T}{\partial y} = T_0 e^{\frac{2x}{L}} \theta'(\eta) \frac{\partial \left(y \sqrt{\frac{a}{2L\theta_f}} e^{\frac{x}{2L}} \right)}{\partial y}$$

$$\frac{\partial T}{\partial y} = \sqrt{\frac{a}{2L\theta_f}} e^{\frac{x}{2L}} T_0 e^{\frac{2x}{L}} \theta'(\eta)$$

$$\frac{\partial T}{\partial y} = \sqrt{\frac{a}{2L\theta_f}} T_0 e^{\frac{5x}{2L}} \theta'(\eta) \tag{A.13}$$

Again

$$\frac{\partial^2 T}{\partial y^2} = \sqrt{\frac{a}{2L\theta_f}} T_0 e^{\frac{5x}{2L}} \frac{\partial \theta'(\eta)}{\partial y}$$

$$\frac{\partial^2 T}{\partial y^2} = \sqrt{\frac{a}{2L\theta_f}} T_0 e^{\frac{5x}{2L}} \theta''(\eta) \frac{\partial \left(y \sqrt{\frac{a}{2L\theta_f}} e^{\frac{x}{2L}} \right)}{\partial y}$$

$$\frac{\partial^2 T}{\partial y^2} = \frac{a}{2L\theta_f} T_0 e^{\frac{3x}{L}} \theta''(\eta) \tag{A.14}$$

By substituting (A.1), (A.2) and (A.12) – (A.14) into equation (8.3), we get:

$$\begin{aligned} & a e^{\frac{x}{L}} f'(\eta) \frac{T_0}{2L} e^{\frac{2x}{L}} (4\theta(\eta) + \eta \cdot \theta'(\eta)) \\ & - \sqrt{\frac{a\theta_f}{2L}} e^{\frac{x}{2L}} [f(\eta) + \eta f'(\eta)] \sqrt{\frac{a}{2L\theta_f}} T_0 e^{\frac{5x}{2L}} \theta'(\eta) \\ & = \frac{1}{(\rho C_p)_{nf}} \left[k_{nf} \left(1 + \frac{16T_\infty^3 \sigma^*}{3k_{nf} k^*} \right) \frac{a}{2L\theta_f} T_0 e^{\frac{3x}{L}} \theta \theta''(\eta) + Q T_0 e^{\frac{2x}{L}} \theta(\eta) \right] \end{aligned}$$

$$\begin{aligned}
& a e^{\frac{x}{L}} f'(\eta) \frac{T_0}{2L} e^{\frac{2x}{L}} (4\theta(\eta) + \eta \cdot \theta'(\eta)) \\
& - \sqrt{\frac{a\vartheta_f}{2L}} e^{\frac{x}{2L}} [f(\eta) + \eta f'(\eta)] \sqrt{\frac{a}{2L\vartheta_f}} T_0 e^{\frac{5x}{2L}} \theta'(\eta) \\
& = \frac{1}{(\rho C_p)_{nf}} \left[k_{nf} \left(1 + \frac{16T_\infty^3 \sigma^*}{3k_{nf} k^* f} \right) \frac{a}{2L\vartheta_f} T_0 e^{\frac{3x}{L}} \theta \theta''(\eta) + QT_0 e^{\frac{2x}{L}} \theta(\eta) \right]
\end{aligned}$$

$$\begin{aligned}
& \frac{aT_0}{2L} e^{\frac{3x}{L}} \{4f'(\eta) \cdot \theta(\eta) - f(\eta)\theta'(\eta)\} \\
& = \frac{aT_0}{2L} e^{\frac{3x}{L}} \frac{1}{(\rho C_p)_{nf}} \left[\frac{k_{nf}}{\vartheta_f} \left(1 + \frac{4Rd}{3} \right) \theta''(\eta) + \frac{2LQ}{ae^{\frac{x}{L}}} \theta(\eta) \right]
\end{aligned}$$

Where $Rd = \frac{4T_\infty^3 \sigma^*}{k_{nf} k^* f}$, more simplification the above equation takes the form

$$\begin{aligned}
& \{4f'(\eta) \cdot \theta(\eta) - f(\eta)\theta'(\eta)\} \\
& = \frac{1}{(\rho C_p)_f \left(1 - \phi + \phi \frac{(\rho C_p)_s}{(\rho C_p)_f} \right)} \left[\frac{k_{nf}}{\vartheta_f} \left(1 + \frac{4Rd}{3} \right) \theta''(\eta) + \frac{2LQ}{ae^{\frac{x}{L}}} \theta(\eta) \right]
\end{aligned}$$

$$\begin{aligned}
& \{4f'(\eta) \cdot \theta(\eta) - f(\eta)\theta'(\eta)\} \\
& = \frac{1}{\left(1 - \phi + \phi \frac{(\rho C_p)_s}{(\rho C_p)_f} \right)} \left[\frac{k_{nf}}{\vartheta_f} \frac{1}{(\rho C_p)_f} \left(1 + \frac{4Rd}{3} \right) \theta''(\eta) \right. \\
& \quad \left. + \frac{2LQ}{(\rho C_p)_f ae^{\frac{x}{L}}} \theta(\eta) \right]
\end{aligned}$$

$$\{4f'(\eta) \cdot \theta(\eta) - f(\eta)\theta'(\eta)\}$$

$$= \frac{1}{\left(1 - \phi + \phi \frac{(\rho c_p)_s}{(\rho c_p)_f}\right)} \left[\frac{k_{nf}}{k_f} \frac{1}{Pr} \left(1 + \frac{4Rd}{3}\right) \theta''(\eta) + 2\chi\theta(\eta) \right]$$

Where, $Pr = \frac{(\rho c_p)_f \vartheta_f}{k_f}$ $\chi = \frac{LQ}{(\rho c_p)_f a e \bar{L}} = \frac{LQ}{(\rho c_p)_f u_w}$

$$\frac{k_{nf}}{k_f} \frac{1}{Pr} \left(1 + \frac{4Rd}{3}\right) \theta''(\eta) + \left(1 - \phi + \phi \frac{(\rho c_p)_s}{(\rho c_p)_f}\right) (f(\eta)\theta'(\eta) - 4f'(\eta) \cdot \theta(\eta))$$

$$+ 2\chi\theta(\eta) = 0$$

$$\left(1 + \frac{4Rd}{3}\right) \theta'' + Pr \frac{k_f}{k_{nf}} \left\{ \left(1 - \phi + \phi \frac{(\rho c_p)_s}{(\rho c_p)_f}\right) (f\theta' - 4f'\theta) + 2\chi\theta \right\} = 0$$

Boundary condition

$$v = v_w; u = \lambda u_w(x) + A \frac{\partial u}{\partial y}; T = T_w + D \frac{\partial T}{\partial y}; \quad \text{at } y = 0$$

$$u \rightarrow 0; T \rightarrow T_\infty; \quad \text{as } y \rightarrow \infty$$

The similarity equations for boundary conditions (A. 4) by the following substitution.

For the boundary condition at $y = 0 \Rightarrow \eta = y \sqrt{\frac{U_w}{2\theta l}} e^{x/2} = 0$

$$v = v_w;$$

$$-\sqrt{\frac{a\vartheta_f}{2L}} e^{\frac{x}{2L}} [f(\eta) + \eta f'(\eta)], = -\sqrt{\frac{a\vartheta_f}{2L}} e^{\frac{x}{2L}S}$$

$$[f(\eta) + \eta f'(\eta)] = S$$

$$f(0) = S \quad \eta = 0$$

$$u = \lambda u_w(x) + A \frac{\partial u}{\partial y}$$

$$ae^{\frac{x}{2L}} f'(\eta) = \lambda ae^{\frac{x}{2L}} + Aa \sqrt{\frac{a}{2L\theta_f}} e^{\frac{3x}{2L}} f''(\eta)$$

$$f'(\eta) = \lambda + A \sqrt{\frac{a}{2L\theta_f}} e^{\frac{x}{2L}} f''(\eta)$$

$$f'(\eta) = \lambda + \delta f''(\eta)$$

$$\text{Where, } \delta = A \sqrt{\frac{a}{2L\theta_f}} e^{\frac{x}{2L}}$$

$$f'(0) = \lambda + \delta f''(0), \quad \eta = 0$$

$$T = T_w + D \frac{\partial T}{\partial y};$$

$$T_\infty + (T_w - T_\infty)\theta(\eta) = T_w + D \sqrt{\frac{a}{2L\theta}} T_0 e^{\frac{5x}{2L}} \theta'(\eta)$$

$$(T_w - T_\infty)\theta(\eta) = (T_w - T_\infty) + D \sqrt{\frac{a}{2L\theta_f}} T_0 e^{\frac{5x}{2L}} \theta'(\eta)$$

$$T_0 e^{\frac{2x}{L}} \theta(\eta) = T_0 e^{\frac{2x}{L}} + D \sqrt{\frac{a}{2L\theta_f}} T_0 e^{\frac{5x}{2L}} \theta'(\eta)$$

$$\theta(\eta) = 1 + \frac{D \sqrt{\frac{a}{2L\vartheta_f}} e^{\frac{5x}{2L}}}{e^{\frac{2x}{L}}} \theta'(\eta)$$

$$\theta(\eta) = 1 + D \sqrt{\frac{a}{2L\vartheta_f}} e^{\frac{x}{2L}} \theta'(\eta)$$

$$\theta(\eta) = 1 + \delta_T \theta'(\eta)$$

$$\text{Where, } \delta_T = D \sqrt{\frac{a}{2L\vartheta_f}} e^{\frac{x}{2L}}$$

$$\theta(0) = 1 + \delta_T \theta'(0) \text{ at } \eta = 0$$

For the boundary condition as $y \rightarrow \infty \Rightarrow \eta = y \sqrt{\frac{U_w}{2\vartheta l}} e^{x/2} \rightarrow \infty$

$$u \rightarrow 0$$

$$ae^{\frac{x}{2L}} f'(\eta) \rightarrow 0$$

$$f'(\eta) \rightarrow 0 \text{ as } \eta \rightarrow \infty$$

$$T \rightarrow T_\infty$$

$$T \rightarrow T_\infty$$

$$T_\infty + (T_w - T_\infty)\theta(\eta) \rightarrow T_\infty$$

$$(T_w - T_\infty)\theta(\eta) \rightarrow 0$$

$$\theta(\eta) \rightarrow 0 \text{ as } \eta \rightarrow \infty$$

Therefore, by using transformations (6.5) in Equations (8.2) – (8.4) we get,

$$\left(1 + \frac{1}{\beta}\right) f''' + (1 - \phi)^{2.5} \left[\left(1 - \phi + \phi \left(\frac{\rho_s}{\rho_f}\right)\right) (ff'' - 2f'^2) \right] + 2\zeta \left(1 - \phi + \phi \frac{(\rho\beta)_s}{(\rho\beta)_f}\right) \theta = 0 \quad (8.5)$$

$$\left(1 + \frac{4Rd}{3}\right) \theta'' + Pr \frac{k_f}{k_{nf}} \left\{ \left(1 - \phi + \phi \frac{(\rho c_p)_s}{(\rho c_p)_f}\right) (f\theta' - 4f'\theta) + 2\chi\theta \right\} = 0 \quad (8.6)$$

and the boundary conditions

$$f(0) = S; \quad f'(0) = \lambda + \delta f''(0); \quad \theta(0) = 1 + \delta_T \theta'(0),$$

$$f'(\eta) \rightarrow 0; \quad \theta(\eta) \rightarrow 0; \quad \text{as } \eta \rightarrow \infty \quad (8.7)$$



UUM
Universiti Utara Malaysia

APPENDIX B

DERIVATIONS OF THE STABILITY ANALYSIS

To perform the stability analysis, the governing equations of the momentum and heat transfer (8.2) and (8.3) are written into unsteady form as

$$\begin{aligned} \frac{\partial u}{\partial t} + u \frac{\partial u}{\partial x} + v \frac{\partial u}{\partial y} \\ = \frac{1}{\rho_{nf}} \left[\mu_{nf} \left(1 + \frac{1}{\beta} \right) \frac{\partial^2 u}{\partial y^2} + g(\rho\beta\tau)_{nf}(T - T_{\infty}) \right] \end{aligned} \quad (8.8)$$

$$\begin{aligned} \frac{\partial T}{\partial t} + u \frac{\partial T}{\partial x} + v \frac{\partial T}{\partial y} \\ = \frac{1}{(\rho C_p)_{nf}} \left[k_{nf} \left(1 + \frac{16T_{\infty}^3 \sigma^*}{3k_{nf} k^*} \right) \frac{\partial^2 T}{\partial y^2} + Q(T - T_{\infty}) \right] \end{aligned} \quad (8.9)$$

Similarity transformations are given in (6.5) are extended with new dimensionless time dependent variable τ like as

$$\begin{aligned} \psi = \sqrt{2a\vartheta L} e^{\frac{x}{2L}} f(\eta, \tau); \theta(\eta, \tau) = \frac{T - T_{\infty}}{T_w - T_{\infty}}; \\ \eta = y \sqrt{\frac{a}{2L\vartheta_f}} e^{\frac{x}{2L}}; \tau = \frac{a}{2l} e^{x/l} t \end{aligned} \quad (6.12)$$

The velocity component u and v take the following forms

$$u = a e^{\frac{x}{2L}} \frac{\partial f(\eta, \tau)}{\partial \eta}; \quad v = -\sqrt{\frac{a\vartheta_f}{2L}} e^{\frac{x}{2L}} \left[f(\eta, \tau) + \eta \frac{\partial f(\eta, \tau)}{\partial \eta} \right] \quad (B.1)$$

To get the similarity solution of the momentum Equation (B.1). $\frac{\partial u}{\partial t}$, $\frac{\partial u}{\partial y}$, $\frac{\partial^2 u}{\partial y^2}$ and $g(\rho\beta\tau)_{nf}(T - T_{\infty})$ are needed to be find out. Therefore,

$$\frac{\partial u}{\partial y} = ae^{\frac{x}{L}} \left(\frac{\partial^2 f(\eta, \tau)}{\partial \eta^2} \frac{\partial \left(y \sqrt{\frac{a}{2L\theta}} e^{\frac{x}{2L}} \right)}{\partial y} + \frac{\partial^2 f(\eta, \tau)}{\partial \eta \partial \tau} \frac{\partial \left(\frac{a}{2L} e^{x/lt} \right)}{\partial y} \right)$$

$$\frac{\partial u}{\partial y} = ae^{\frac{x}{L}} \left(\sqrt{\frac{a}{2L\theta_f}} e^{\frac{3x}{2L}} \frac{\partial^2 f(\eta, \tau)}{\partial \eta^2} + (0) \right)$$

$$\frac{\partial u}{\partial y} = a \sqrt{\frac{a}{2L\theta_f}} e^{\frac{3x}{2L}} \frac{\partial^2 f(\eta, \tau)}{\partial \eta^2} \quad (\text{B.4})$$

$$\frac{\partial^2 u}{\partial y^2} = a \sqrt{\frac{a}{2L\theta_f}} e^{\frac{3x}{2L}} \frac{\partial}{\partial y} \left(\frac{\partial^2 f(\eta, \tau)}{\partial \eta^2} \right)$$

$$\frac{\partial^2 u}{\partial y^2} = a \sqrt{\frac{a}{2L\theta_f}} e^{\frac{3x}{2L}} \frac{\partial}{\partial y} \left(\frac{\partial^2 f(\eta, \tau)}{\partial \eta^2} \right)$$

$$\frac{\partial^2 u}{\partial y^2} = a \sqrt{\frac{a}{2L\theta_f}} e^{\frac{3x}{2L}} \left(\frac{\partial^3 f(\eta, \tau)}{\partial \eta^3} \frac{\partial \left(y \sqrt{\frac{a}{2L\theta}} e^{\frac{x}{2L}} \right)}{\partial y} + \frac{\partial^3 f(\eta, \tau)}{\partial \eta^3} \frac{\partial \left(\frac{a}{2L} e^{x/lt} \right)}{\partial y} \right)$$

$$\frac{\partial^2 u}{\partial y^2} = a \sqrt{\frac{a}{2L\theta_f}} e^{\frac{3x}{2L}} \left(\sqrt{\frac{a}{2L\theta}} e^{\frac{x}{2L}} \frac{\partial^3 f(\eta, \tau)}{\partial \eta^3} + \frac{\partial^3 f(\eta, \tau)}{\partial \eta^3} (0) \right)$$

$$\frac{\partial^2 u}{\partial y^2} = \frac{a^2}{2L\theta_f} e^{\frac{2x}{L}} \frac{\partial^3 f(\eta, \tau)}{\partial \eta^3} \quad (\text{B.5})$$

By substituting (B.1) -(B.5) in Equation (8.11), we get

$$\begin{aligned}
& \frac{a^2}{2l} e^{\frac{2x}{L}} \frac{\partial^2 f(\eta, \tau)}{\partial \eta \partial \tau} + a e^{\frac{x}{L}} \frac{\partial f(\eta, \tau)}{\partial \eta} \left(\frac{a}{2L} e^{\frac{x}{L}} \left[2 \frac{\partial f(\eta, \tau)}{\partial \eta} + \eta \frac{\partial^2 f(\eta, \tau)}{\partial \eta^2} + 2\tau \frac{\partial^2 f(\eta, \tau)}{\partial \eta \partial \tau} \right] \right) \\
& - \sqrt{\frac{a \vartheta_f}{2L}} e^{\frac{x}{2L}} \left[f(\eta, \tau) + \eta \frac{\partial f(\eta, \tau)}{\partial \eta} \right] \left(a \sqrt{\frac{a}{2L \vartheta}} e^{\frac{3x}{2L}} \frac{\partial^2 f(\eta, \tau)}{\partial \eta^2} \right) \\
& = \frac{1}{\rho_{nf}} \left[\mu_{nf} \left(1 + \frac{1}{\beta} \right) \frac{a^2}{2L \vartheta} e^{\frac{2x}{L}} \frac{\partial^3 f(\eta, \tau)}{\partial \eta^3} + g(\rho \beta_T)_{nf} T_0 e^{\frac{2x}{L}} \theta(\eta, \tau) \right] \\
& \frac{a^2}{2l} e^{\frac{2x}{L}} \frac{\partial^2 f(\eta, \tau)}{\partial \eta \partial \tau} + \frac{a^2}{2L} e^{\frac{2x}{L}} \frac{\partial f(\eta, \tau)}{\partial \eta} \left[2 \frac{\partial f(\eta, \tau)}{\partial \eta} + \eta \frac{\partial^2 f(\eta, \tau)}{\partial \eta^2} + 2\tau \frac{\partial^2 f(\eta, \tau)}{\partial \eta \partial \tau} \right] \\
& - \frac{a^2}{2L} e^{\frac{2x}{L}} \frac{\partial^2 f(\eta, \tau)}{\partial \eta^2} \left[f(\eta, \tau) + \eta \frac{\partial f(\eta, \tau)}{\partial \eta} \right] \\
& = \frac{a^2}{2L} e^{\frac{2x}{L}} \left[\frac{\mu_{nf}}{\vartheta_f \rho_{nf}} \left(1 + \frac{1}{\beta} \right) \frac{\partial^3 f(\eta, \tau)}{\partial \eta^3} + \frac{2Lg(\rho \beta_T)_{nf} T_0}{\rho_{nf} a^2} \theta(\eta, \tau) \right]
\end{aligned}$$

After simplification, we have

$$\begin{aligned}
& \frac{\partial^2 f(\eta, \tau)}{\partial \eta \partial \tau} + \frac{\partial f(\eta, \tau)}{\partial \eta} \left[2 \frac{\partial f(\eta, \tau)}{\partial \eta} + \eta \frac{\partial^2 f(\eta, \tau)}{\partial \eta^2} + 2\tau \frac{\partial^2 f(\eta, \tau)}{\partial \eta \partial \tau} \right] \\
& - \frac{\partial^2 f(\eta, \tau)}{\partial \eta^2} \left[f(\eta, \tau) + \eta \frac{\partial f(\eta, \tau)}{\partial \eta} \right] \\
& = \left[\frac{\mu_{nf}}{\vartheta_f \rho_{nf}} \left(1 + \frac{1}{\beta} \right) \frac{\partial^3 f(\eta, \tau)}{\partial \eta^3} + \frac{2Lg(\rho \beta_T)_{nf} T_0}{\rho_{nf} a^2} \theta(\eta, \tau) \right]
\end{aligned}$$

$$\begin{aligned} & \frac{\partial^2 f(\eta, \tau)}{\partial \eta \partial \tau} + \left[2 \left(\frac{\partial f(\eta, \tau)}{\partial \eta} \right)^2 + \eta \frac{\partial^2 f(\eta, \tau)}{\partial \eta^2} \frac{\partial f(\eta, \tau)}{\partial \eta} + 2\tau \frac{\partial^2 f(\eta, \tau)}{\partial \eta \partial \tau} \frac{\partial f(\eta, \tau)}{\partial \eta} \right] \\ & - \left[f(\eta, \tau) \frac{\partial^2 f(\eta, \tau)}{\partial \eta^2} + \eta \frac{\partial^2 f(\eta, \tau)}{\partial \eta^2} \frac{\partial f(\eta, \tau)}{\partial \eta} \right] \\ & = \frac{1}{\left((1-\phi) + \phi \left(\frac{\rho_s}{\rho_f} \right) \right)} \left[\frac{1}{(1-\phi)^{2.5}} \left(1 + \frac{1}{\beta} \right) \frac{\partial^3 f(\eta, \tau)}{\partial \eta^3} \right. \\ & \left. + 2\zeta \left((1-\phi) + \phi \frac{(\rho\beta\tau)_s}{(\rho\beta\tau)_f} \right) \theta(\eta, \tau) \right] \end{aligned}$$

$$\begin{aligned} & \frac{\partial^2 f(\eta, \tau)}{\partial \eta \partial \tau} + \left[2 \left(\frac{\partial f(\eta, \tau)}{\partial \eta} \right)^2 - f(\eta, \tau) \frac{\partial^2 f(\eta, \tau)}{\partial \eta^2} + 2\tau \frac{\partial^2 f(\eta, \tau)}{\partial \eta \partial \tau} \frac{\partial f(\eta, \tau)}{\partial \eta} \right] \\ & = \frac{1}{\left((1-\phi) + \phi \left(\frac{\rho_s}{\rho_f} \right) \right)} \left[\frac{1}{(1-\phi)^{2.5}} \left(1 + \frac{1}{\beta} \right) \frac{\partial^3 f(\eta, \tau)}{\partial \eta^3} \right. \\ & \left. + 2\zeta \left((1-\phi) + \phi \frac{(\rho\beta\tau)_s}{(\rho\beta\tau)_f} \right) \theta(\eta, \tau) \right] \end{aligned}$$

$$\begin{aligned} & \frac{1}{\left((1-\phi) + \phi \left(\frac{\rho_s}{\rho_f} \right) \right)} \left[\frac{1}{(1-\phi)^{2.5}} \left(1 + \frac{1}{\beta} \right) \frac{\partial^3 f(\eta, \tau)}{\partial \eta^3} \right. \\ & \left. + 2\zeta \left((1-\phi) + \phi \frac{(\rho\beta\tau)_s}{(\rho\beta\tau)_f} \right) \theta(\eta, \tau) \right] + f(\eta, \tau) \frac{\partial^2 f(\eta, \tau)}{\partial \eta^2} \\ & - 2 \left(\frac{\partial f(\eta, \tau)}{\partial \eta} \right)^2 - 2\tau \frac{\partial^2 f(\eta, \tau)}{\partial \eta \partial \tau} \frac{\partial f(\eta, \tau)}{\partial \eta} - \frac{\partial^2 f(\eta, \tau)}{\partial \eta \partial \tau} = 0 \quad (B.6) \end{aligned}$$

The boundary conditions become

$$f(0, \tau) = S; \frac{\partial f(0, \tau)}{\partial \eta} = \lambda + \delta \frac{\partial^2 f(0, \tau)}{\partial \eta^2}; \text{ at } \eta = 0$$

$$\frac{\partial f(\eta, \tau)}{\partial \eta} \rightarrow 0; \text{ as } \eta \rightarrow \infty$$
(B.7)

To test the stability of the steady flow solution of $f(\eta) = f_0(\eta)$

We will write,

$$f(\eta) = f_0(\eta) + e^{-\varepsilon\tau} F(\eta, \tau)$$
(B.8)

Where, $0 < F(\eta, \tau) \ll 1$, ε is unknown eigenvalue and $F(\eta, \tau)$ is a smallest relative to $f(\eta) = f_0(\eta)$

Therefore, differentiating according to the need of the equation as follows

$$\frac{\partial f(\eta, \tau)}{\partial \eta} = \frac{df_0}{d\eta} + e^{-\varepsilon\tau} \frac{dF}{d\eta}; \frac{\partial^2 f(\eta, \tau)}{\partial \eta^2} = \frac{d^2 f_0}{d\eta^2} + e^{-\varepsilon\tau} \frac{d^2 F}{d\eta^2}$$

$$\frac{\partial^2 f(\eta, \tau)}{\partial \tau \partial \eta} = -\varepsilon e^{-\varepsilon\tau} \frac{dF}{d\eta}; \frac{\partial^3 f(\eta, \tau)}{\partial \eta^3} = \frac{d^3 f_0}{d\eta^3} + e^{-\varepsilon\tau} \frac{d^3 F}{d\eta^3}$$
(B.9)

By substituting (B.9) into (B.6), It is obtained

$$\frac{1}{\left((1 - \phi) + \phi \left(\frac{\rho_s}{\rho_f} \right) \right)} \left[\frac{1}{(1 - \phi)^{2.5}} \left(1 + \frac{1}{\beta} \right) \left(\frac{d^3 f_0}{d\eta^3} + e^{-\varepsilon\tau} \frac{d^3 F}{d\eta^3} \right) \right.$$

$$\left. + 2\zeta \left((1 - \phi) + \phi \left(\frac{\rho\beta\tau}{\rho\beta\tau} \right)_s \right) (\theta_0(\eta) + e^{-\varepsilon\tau} G(\eta, 0)) \right]$$

$$+ (f_0 + e^{-\varepsilon\tau} F) \left(\frac{d^2 f_0}{d\eta^2} + e^{-\varepsilon\tau} \frac{d^2 F}{d\eta^2} \right) - 2 \left(\frac{df_0}{d\eta} + e^{-\varepsilon\tau} \frac{dF}{d\eta} \right)^2$$

$$- 2\tau \left(-\varepsilon e^{-\varepsilon\tau} \frac{dF}{d\eta} \right) \left(\frac{df_0}{d\eta} + e^{-\varepsilon\tau} \frac{dF}{d\eta} \right) + \varepsilon e^{-\varepsilon\tau} \frac{dF}{d\eta} = 0$$

$$\begin{aligned} & \frac{1}{\left((1-\phi) + \phi \left(\frac{\rho_s}{\rho_f} \right) \right)} \left[\frac{1}{(1-\phi)^{2.5}} \left(1 + \frac{1}{\beta} \right) \left(\frac{d^3 f_0}{d\eta^3} + e^{-\varepsilon\tau} \frac{d^3 F}{d\eta^3} \right) \right. \\ & \quad \left. + 2\zeta \left((1-\phi) + \phi \frac{(\rho\beta_T)_s}{(\rho\beta_T)_f} \right) (\theta_0(\eta) + e^{-\varepsilon\tau} G(\eta, 0)) \right] \\ & \quad + (f_0 + e^{-\varepsilon\tau} F) \left(\frac{d^2 f_0}{d\eta^2} + e^{-\varepsilon\tau} \frac{d^2 F}{d\eta^2} \right) - 2 \left(\frac{df_0}{d\eta} + e^{-\varepsilon\tau} \frac{dF}{d\eta} \right)^2 \\ & \quad - 2\tau \left(-\varepsilon e^{-\varepsilon\tau} \frac{dF}{d\eta} \right) \left(\frac{df_0}{d\eta} + e^{-\varepsilon\tau} \frac{dF}{d\eta} \right) + \varepsilon e^{-\varepsilon\tau} \frac{dF}{d\eta} = 0 \end{aligned}$$

$$\begin{aligned} & \left[\frac{1}{\left((1-\phi) + \phi \left(\frac{\rho_s}{\rho_f} \right) \right) (1-\phi)^{2.5}} \left(1 + \frac{1}{\beta} \right) \frac{d^3 f_0}{d\eta^3} + f_0 \frac{d^2 f_0}{d\eta^2} - 2 \left(\frac{df_0}{d\eta} \right)^2 \right. \\ & \quad \left. + 2\zeta \frac{\left((1-\phi) + \phi \frac{(\rho\beta_T)_s}{(\rho\beta_T)_f} \right)}{\left((1-\phi) + \phi \left(\frac{\rho_s}{\rho_f} \right) \right)} \theta_0(\eta) \right] \\ & \quad + e^{-\varepsilon\tau} \left[\frac{1}{\left((1-\phi) + \phi \left(\frac{\rho_s}{\rho_f} \right) \right) (1-\phi)^{2.5}} \left(1 + \frac{1}{\beta} \right) \frac{d^3 F}{d\eta^3} + f_0 \frac{d^2 F}{d\eta^2} \right. \\ & \quad \left. + F \frac{d^2 f_0}{d\eta^2} - 4 \frac{df_0}{d\eta} \frac{dF}{d\eta} + 2\tau\varepsilon \frac{dF}{d\eta} \frac{df_0}{d\eta} \right. \\ & \quad \left. + 2\zeta \frac{\left((1-\phi) + \phi \frac{(\rho\beta_T)_s}{(\rho\beta_T)_f} \right)}{\left((1-\phi) + \phi \left(\frac{\rho_s}{\rho_f} \right) \right)} G(\eta, \tau) + \varepsilon \frac{dF}{d\eta} \right] \\ & \quad + e^{-2\varepsilon\tau} \left[F \frac{d^2 F}{d\eta^2} - 2 \left(\frac{dF}{d\eta} \right)^2 + 2\tau \left(\frac{dF}{d\eta} \right)^2 \right] = 0 \end{aligned}$$

As it is mentioned that $f(\eta) = f_0(\eta)$ which means that the terms only contain $f_0(\eta)$ show the steady state solution. In this case, we have following terms

$$\left[\frac{1}{\left((1-\phi) + \phi \left(\frac{\rho_s}{\rho_f} \right) \right) (1-\phi)^{2.5}} \left(1 + \frac{1}{\beta} \right) \frac{d^3 f_0}{d\eta^3} + f_0 \frac{d^2 f_0}{d\eta^2} - 2 \left(\frac{df_0}{d\eta} \right)^2 + 2\zeta \frac{\left((1-\phi) + \phi \left(\frac{\rho\beta_T}{\rho\beta_T} \right)_s \right)}{\left((1-\phi) + \phi \left(\frac{\rho_s}{\rho_f} \right) \right)} \theta_0(\eta) \right]$$

For the stability analysis, only remaining terms which multiple of the $e^{-\varepsilon\tau}$ will be examined,

$$e^{-\varepsilon\tau} \left[\frac{1}{\left((1-\phi) + \phi \left(\frac{\rho_s}{\rho_f} \right) \right) (1-\phi)^{2.5}} \left(1 + \frac{1}{\beta} \right) \frac{d^3 F}{d\eta^3} + f_0 \frac{d^2 F}{d\eta^2} + F \frac{d^2 f_0}{d\eta^2} - 4 \frac{df_0}{d\eta} \frac{dF}{d\eta} + 2\tau \varepsilon \frac{dF}{d\eta} \frac{df_0}{d\eta} + 2\zeta \frac{\left((1-\phi) + \phi \left(\frac{\rho\beta_T}{\rho\beta_T} \right)_s \right)}{\left((1-\phi) + \phi \left(\frac{\rho_s}{\rho_f} \right) \right)} G(\eta, \tau) + \varepsilon \frac{dF}{d\eta} \right] + e^{-2\varepsilon\tau} \left[F \frac{d^2 F}{d\eta^2} - 2 \left(\frac{dF}{d\eta} \right)^2 + 2\tau \left(\frac{dF}{d\eta} \right)^2 \right] = 0 \quad (B.10)$$

By keeping $\tau = 0$, we have the following linearized equation:

$$\left(1 + \frac{1}{\beta} \right) F_0''' + (1-\phi)^{2.5} \left[\left((1-\phi) + \phi \left(\frac{\rho_s}{\rho_f} \right) \right) (f_0 F_0'' + f_0 F_0'' - 4f_0' F_0' + \varepsilon F_0') + 2\zeta \left((1-\phi) + \phi \left(\frac{\rho\beta_T}{\rho\beta_T} \right)_s \right) G_0 \right] = 0 \quad (B.11)$$

And the boundary conditions for momentum equations are transferred as

$$f(0, \tau) = S$$

$$f_0(0) + e^{-\varepsilon t} F(0, \tau) = S$$

$$S + e^{-\varepsilon t} F(0, \tau) = S$$

$$e^{-\varepsilon t} F(0, \tau) = 0$$

By keeping $\tau = 0$

$$F_0(0) = 0$$

$$\frac{\partial f(0)}{\partial \eta} = \lambda + \delta \frac{\partial^2 f(0, \tau)}{\partial \eta^2}$$

$$\frac{df_0(0)}{d\eta} + e^{-\varepsilon t} \frac{dF(0, \tau)}{d\eta} = \lambda + \delta \left(\frac{d^2 f_0(0)}{d\eta^2} + e^{-\varepsilon t} \frac{d^2 F(0, \tau)}{d\eta^2} \right)$$

By substituting $\tau = 0$, we have

$$\frac{df_0(0)}{d\eta} + e^{-\varepsilon 0} \frac{dF(0, 0)}{d\eta} = \lambda + \delta \left(\frac{d^2 f_0(0)}{d\eta^2} \right) + e^{-\varepsilon 0} \delta \left(\frac{d^2 F(0, 0)}{d\eta^2} \right)$$

$$f'_0(0) + F'_0(0) = \lambda + \delta f''_0(0) + \delta F''_0(0)$$

$$\lambda + \delta f''_0(0) + F'_0(0) = \lambda + \delta f''_0(0) + \delta F''_0(0) \text{ where } f'_0(0) = \lambda + \delta f''_0(0)$$

$$F'_0(0) = \delta F''_0(0)$$

$$\frac{\partial f(\eta, \tau)}{\partial \eta} \rightarrow 0 \text{ as } \eta \rightarrow \infty$$

$$\left(\frac{df_0(\eta)}{d\eta} + e^{-\varepsilon t} \frac{dF(\eta, \tau)}{d\eta} \right) \rightarrow 0$$

By substituting $\tau = 0$, we have

$$\frac{df_0(\eta)}{d\eta} + e^{-\varepsilon_0} \frac{dF(\eta, 0)}{d\eta} \rightarrow 0$$

$$f_0'(\eta) + F_0'(\eta, 0) \rightarrow 0$$

$$0 + F_0'(\eta, 0) \rightarrow 0 \text{ where } f_0'(\eta) \rightarrow 0 \text{ as } \eta \rightarrow \infty$$

$$F_0'(\eta, 0) \rightarrow 0, \text{ as } \eta \rightarrow \infty$$

It can be written as

$$F_0'(\eta) \rightarrow 0, \text{ as } \eta \rightarrow \infty$$

To obtain stability analysis of heat transfer Equation (8.9), $\frac{\partial T}{\partial x}$, $\frac{\partial T}{\partial y}$ and $\frac{\partial^2 T}{\partial y^2}$ are required to be find out

For, similarity transformation of heat transfer, we take similarity variable

$$\theta(\eta, \tau) = \frac{(T - T_\infty)}{(T_w - T_\infty)} \quad (\text{B.12})$$

And $T = T_\infty + T_0 e^{\frac{2x}{L}} \theta(\eta, \tau)$; this implies that $T_w = T_\infty + T_0 e^{\frac{2x}{L}}$,

Therefore, we have

$$\frac{\partial T}{\partial t} = \frac{\partial}{\partial t} \left(T_\infty + T_0 e^{\frac{2x}{L}} \theta(\eta, \tau) \right),$$

$$\frac{\partial T}{\partial t} = 0 + T_0 e^{\frac{2x}{L}} \frac{\partial \theta(\eta, \tau)}{\partial \tau} \frac{\partial \tau}{\partial t}$$

$$\frac{\partial T}{\partial t} = T_0 e^{\frac{2x}{L}} \frac{\partial \theta(\eta, \tau)}{\partial \tau} \frac{\partial \left(\frac{a}{2L} e^{x/lt} \right)}{\partial t}$$

$$\frac{\partial T}{\partial t} = \frac{a T_0}{2l} e^{\frac{3x}{L}} \frac{\partial \theta(\eta, \tau)}{\partial \tau} \quad (B.13)$$

$$\frac{\partial T}{\partial x} = \frac{\partial}{\partial x} \left(T_\infty + T_0 e^{\frac{2x}{L}} \theta(\eta, \tau) \right)$$

$$\frac{\partial T}{\partial x} = T_0 \left(\frac{2}{L} e^{\frac{2x}{L}} \theta(\eta, \tau) + e^{\frac{2x}{L}} \left\{ \frac{\partial \theta(\eta, \tau)}{\partial \eta} \frac{\partial \eta}{\partial x} + \frac{\partial \theta(\eta, \tau)}{\partial \tau} \frac{\partial \tau}{\partial x} \right\} \right)$$

$$\frac{\partial T}{\partial x} = T_0 \left(\frac{2}{L} e^{\frac{2x}{L}} \theta(\eta, \tau) + e^{\frac{2x}{L}} \left\{ \frac{\partial \theta(\eta, \tau)}{\partial \eta} \frac{\partial \left(y \sqrt{\frac{a}{2L\vartheta}} e^{\frac{x}{2L}} \right)}{\partial x} + \frac{\partial \theta(\eta, \tau)}{\partial \tau} \frac{\partial \left(\frac{a}{2l} e^{x/lt} \right)}{\partial x} \right\} \right)$$

$$\frac{\partial T}{\partial x} = T_0 \left(\frac{2}{L} e^{\frac{2x}{L}} \theta(\eta, \tau) + \frac{1}{2L} e^{\frac{2x}{L}} \frac{\partial \theta(\eta, \tau)}{\partial \eta} \cdot y \sqrt{\frac{a}{2L\vartheta}} e^{\frac{x}{2L}} + \frac{1}{L} \tau e^{\frac{2x}{L}} \frac{\partial \theta(\eta, \tau)}{\partial \tau} \right)$$

$$\frac{\partial T}{\partial x} = T_0 \left(\frac{2}{L} e^{\frac{2x}{L}} \theta(\eta, \tau) + \frac{1}{2L} e^{\frac{2x}{L}} \eta \frac{\partial \theta(\eta, \tau)}{\partial \eta} + \frac{1}{L} \tau e^{\frac{2x}{L}} \frac{\partial \theta(\eta, \tau)}{\partial \tau} \right)$$

$$\frac{\partial T}{\partial x} = \frac{T_0}{2L} e^{\frac{2x}{L}} \left(4\theta(\eta, \tau) + \eta \frac{\partial \theta(\eta, \tau)}{\partial \eta} + 2\tau \frac{\partial \theta(\eta, \tau)}{\partial \tau} \right) \quad (B.14)$$

$$\frac{\partial T}{\partial y} = \frac{\partial}{\partial y} \left(T_\infty + T_0 e^{\frac{2x}{L}} \theta(\eta, \tau) \right)$$

$$\frac{\partial T}{\partial y} = T_0 e^{\frac{2x}{L}} \frac{\partial \theta(\eta, \tau)}{\partial \eta} \frac{\partial \eta}{\partial y}$$

$$\frac{\partial T}{\partial y} = T_0 e^{\frac{2x}{L}} \frac{\partial \theta(\eta, \tau)}{\partial \eta} \frac{\partial \left(y \sqrt{\frac{a}{2L\vartheta}} e^{\frac{x}{2L}} \right)}{\partial y}$$

$$\frac{\partial T}{\partial y} = T_0 \sqrt{\frac{a}{2L\theta}} e^{\frac{5x}{2L}} \frac{\partial \theta(\eta, \tau)}{\partial \eta} \quad (B.15)$$

Now,

$$\frac{\partial^2 T}{\partial y^2} = T_0 \sqrt{\frac{a}{2L\theta}} e^{\frac{5x}{2L}} \frac{\partial^2 \theta(\eta, \tau)}{\partial \eta^2} \frac{\partial \eta}{\partial y}$$

$$\frac{\partial^2 T}{\partial y^2} = T_0 \sqrt{\frac{a}{2L\theta}} e^{\frac{5x}{2L}} \frac{\partial^2 \theta(\eta, \tau)}{\partial \eta^2} \frac{\partial \left(y \sqrt{\frac{a}{2L\theta}} e^{\frac{x}{2L}} \right)}{\partial y}$$

$$\frac{\partial^2 T}{\partial y^2} = \frac{aT_0}{2L\theta} e^{\frac{3x}{L}} \frac{\partial^2 \theta(\eta, \tau)}{\partial \eta^2} \quad (B.16)$$

By substituting velocity components u , v and (A.12) – (A.16) into the Equation(8.9), it is obtained

$$\frac{aT_0}{2L} e^{\frac{3x}{L}} \frac{\partial \theta(\eta, \tau)}{\partial \tau} + ae^{\frac{x}{L}} f'(\eta, \tau) \cdot \frac{T_0}{2L} e^{\frac{2x}{L}} \left(4\theta(\eta, \tau) + \eta \frac{\partial \theta(\eta, \tau)}{\partial \eta} + 2\tau \frac{\partial \theta(\eta, \tau)}{\partial \tau} \right) -$$

$$\sqrt{\frac{a\theta_f}{2L}} e^{\frac{x}{2L}} [f(\eta, \tau) + \eta f'(\eta, \tau)] \cdot T_0 \sqrt{\frac{a}{2L\theta}} e^{\frac{5x}{2L}} \frac{\partial \theta(\eta, \tau)}{\partial \eta} = \frac{aT_0}{2L\theta} e^{\frac{3x}{L}} \frac{k_{nf}}{(\rho C_p)_{nf}} \left(1 +$$

$$\frac{16T_\infty^3 \sigma^*}{3k_{nf} k^* f} \right) \frac{\partial^2 \theta(\eta, \tau)}{\partial \eta^2} - \frac{Q}{(\rho C_p)_{nf}} T_0 e^{\frac{2x}{L}} \theta(\eta, \tau) = 0$$

$$\frac{aT_0}{2L} e^{\frac{3x}{L}} \frac{\partial \theta(\eta, \tau)}{\partial \tau} + \frac{aT_0}{2L} e^{\frac{3x}{L}} f'(\eta, \tau) \left(4\theta(\eta, \tau) + \eta \frac{\partial \theta(\eta, \tau)}{\partial \eta} + 2\tau \frac{\partial \theta(\eta, \tau)}{\partial \tau} \right) - \frac{aT_0}{2L} e^{\frac{3x}{L}} [f(\eta, \tau) +$$

$$\eta f'(\eta, \tau)] \cdot \frac{\partial \theta(\eta, \tau)}{\partial \eta} = \frac{aT_0}{2L} e^{\frac{3x}{L}} \frac{k_{nf}}{\theta_f (\rho C_p)_{nf}} \left(1 + \frac{16T_\infty^3 \sigma^*}{3k_{nf} k^* f} \right) \frac{\partial^2 \theta(\eta, \tau)}{\partial \eta^2} - \frac{Q}{(\rho C_p)_{nf}} T_0 e^{\frac{2x}{L}} \theta(\eta, \tau) = 0$$

Simplifying, we get

$$\frac{\partial \theta(\eta, \tau)}{\partial \tau} + \frac{\partial f(\eta, \tau)}{\partial \eta} \left(4\theta(\eta, \tau) + \eta \frac{\partial \theta(\eta, \tau)}{\partial \eta} + 2\tau \frac{\partial \theta(\eta, \tau)}{\partial \tau} \right) - \left[f(\eta, \tau) + \eta \frac{\partial f(\eta, \tau)}{\partial \eta} \right] \cdot \frac{\partial \theta(\eta, \tau)}{\partial \eta} =$$

$$\frac{k_{nf}}{\rho_f (\rho c_p)_{nf}} \left(1 + \frac{16T_\infty^3 \sigma^*}{3k_{nf} k^* f} \right) \frac{\partial^2 \theta(\eta, \tau)}{\partial \eta^2} - \frac{1}{(\rho c_p)_{nf}} \frac{2LQ}{aeL} \theta(\eta, \tau) = 0$$

Substituting thermo physical properties, we get

$$\frac{1}{\left(1 - \phi + \phi \frac{(\rho c_p)_s}{(\rho c_p)_f} \right)} \frac{1}{(\rho c_p)_f} \frac{k_{nf}}{k_f} \left(1 + \frac{4Rd}{3} \right) \frac{\partial^2 \theta(\eta, \tau)}{\partial \eta^2} - \frac{1}{\left(1 - \phi + \phi \frac{(\rho c_p)_s}{(\rho c_p)_f} \right)} 2 \frac{LQ}{(\rho c_p)_f u_w} \theta(\eta, \tau) -$$

$$4 \frac{\partial f(\eta, \tau)}{\partial \eta} \theta(\eta, \tau) + f(\eta, \tau) \frac{\partial \theta(\eta, \tau)}{\partial \eta} - 2\tau \frac{\partial f(\eta, \tau)}{\partial \eta} \frac{\partial \theta(\eta, \tau)}{\partial \tau} - \frac{\partial \theta(\eta, \tau)}{\partial \tau} = 0$$

$$\frac{1}{\left(1 - \phi + \phi \frac{(\rho c_p)_s}{(\rho c_p)_f} \right)} \frac{1}{Pr} \frac{k_{nf}}{k_f} \left(1 + \frac{4Rd}{3} \right) \frac{\partial^2 \theta(\eta, \tau)}{\partial \eta^2} - \frac{1}{\left(1 - \phi + \phi \frac{(\rho c_p)_s}{(\rho c_p)_f} \right)} 2\chi \theta(\eta, \tau) - 4 \frac{\partial f(\eta, \tau)}{\partial \eta} \theta(\eta, \tau) +$$

$$f(\eta, \tau) \frac{\partial \theta(\eta, \tau)}{\partial \eta} - 2\tau \frac{\partial f(\eta, \tau)}{\partial \eta} \frac{\partial \theta(\eta, \tau)}{\partial \tau} - \frac{\partial \theta(\eta, \tau)}{\partial \tau} = 0$$

As $Pr = \frac{(\rho c_p)_f \theta_f}{k_f}$ and $\chi = \frac{LQ}{(\rho c_p)_f u_w}$

$$\frac{1}{Pr} \frac{k_{nf}}{k_f} \left(1 + \frac{4Rd}{3} \right) \frac{\partial^2 \theta(\eta, \tau)}{\partial \eta^2}$$

$$+ \left(1 - \phi + \phi \frac{(\rho c_p)_s}{(\rho c_p)_f} \right) \left[f(\eta, \tau) \frac{\partial \theta(\eta, \tau)}{\partial \eta} - 4 \frac{\partial f(\eta, \tau)}{\partial \eta} \theta(\eta, \tau) \right.$$

$$\left. - 2\tau \frac{\partial f(\eta, \tau)}{\partial \eta} \frac{\partial \theta(\eta, \tau)}{\partial \tau} - \frac{\partial \theta(\eta, \tau)}{\partial \tau} \right] - 2\chi \theta(\eta, \tau) = 0 \quad (B.17)$$

The transformation in the boundary conditions

$$\theta(0, \tau) = 1 + \delta_\tau \frac{\partial \theta(0, \tau)}{\partial \eta};$$

$$\theta(\eta, \tau) \rightarrow 0; \quad \text{as } \eta \rightarrow \infty$$

In order to test the stability of the steady flow solution $\theta(\eta) = \theta_0(\eta)$,

$$\theta(\eta) = \theta_0(\eta) + e^{-\varepsilon\tau}G(\eta, \tau) \quad (B.18)$$

Where, $0 < G(\eta, \tau) \ll 1$, ε is unknown eigenvalue and $G(\eta, \tau)$ is a smallest relative to $\theta_0(\eta)$

Therefore, differentiating (B.18) according to the requirement of the Equation (B.17)

$$\begin{aligned} \frac{\partial\theta(\eta, \tau)}{\partial\eta} &= \frac{d\theta_0}{d\eta} + e^{-\varepsilon\tau} \frac{dG}{d\eta}, & \frac{\partial^2\theta(\eta, \tau)}{\partial\eta^2} &= \frac{d^2\theta_0}{d\eta^2} + e^{-\varepsilon\tau} \frac{d^2G}{d\eta^2} \\ \frac{\partial\theta(\eta, \tau)}{\partial\tau} &= -\varepsilon e^{-\varepsilon\tau}G \end{aligned} \quad (B.19)$$

Substituting (B.19) in Equation (B.17), we have

$$\begin{aligned} &\frac{1}{Pr} \frac{k_{nf}}{k_f} \left(1 + \frac{4Rd}{3}\right) \left(\frac{d^2\theta_0}{d\eta^2} + e^{-\varepsilon\tau} \frac{d^2G}{d\eta^2}\right) + \left(1 - \phi + \phi \frac{(\rho c_p)_s}{(\rho c_p)_f}\right) \left[f_0(\eta) + \right. \\ &e^{-\varepsilon\tau}F(\eta, \tau) \left. \left(\frac{d\theta_0}{d\eta} + e^{-\varepsilon\tau} \frac{dG}{d\eta}\right) - 4 \left(\frac{df_0}{d\eta} + e^{-\varepsilon\tau} \frac{dF}{d\eta}\right) (\theta_0(\eta) + e^{-\varepsilon\tau}G(\eta, \tau)) - 2\tau \left(\frac{df_0}{d\eta} + \right. \right. \\ &\left. \left. e^{-\varepsilon\tau} \frac{dF}{d\eta}\right) (-\varepsilon e^{-\varepsilon\tau}G) + \varepsilon e^{-\varepsilon\tau}G \right] - 2\chi(\theta_0(\eta) + \varepsilon e^{-\varepsilon\tau}G(\eta, \tau)) = 0 \end{aligned}$$

$$\begin{aligned} &\frac{1}{Pr} \frac{k_{nf}}{k_f} \left(1 + \frac{4Rd}{3}\right) \left(\frac{d^2\theta_0}{d\eta^2} + e^{-\varepsilon\tau} \frac{d^2G}{d\eta^2}\right) + \left(1 - \phi + \phi \frac{(\rho c_p)_s}{(\rho c_p)_f}\right) \left[f_0(\eta) \frac{d\theta_0}{d\eta} + e^{-\varepsilon\tau}f_0(\eta) \frac{dG}{d\eta} + \right. \\ &e^{-\varepsilon\tau}F(\eta, \tau) \frac{d\theta_0}{d\eta} + e^{-2\varepsilon\tau}F(\eta, \tau) \frac{dG}{d\eta} - 4 \frac{df_0}{d\eta} \theta_0(\eta) - 4e^{-\varepsilon\tau} \frac{df_0}{d\eta} G(\eta, \tau) - \\ &4e^{-\varepsilon\tau} \frac{dF}{d\eta} \theta_0(\eta) - 4e^{-2\varepsilon\tau} \frac{dF}{d\eta} G(\eta, \tau) + 2\tau\varepsilon e^{-\varepsilon\tau}G + \varepsilon e^{-\varepsilon\tau}G \left. \right] - 2\beta^*(\theta_0(\eta) + \\ &e^{-\varepsilon\tau}G(\eta, \tau)) = 0 \end{aligned}$$

$$\left[\frac{1}{Pr} \frac{k_{nf}}{k_f} \left(1 + \frac{4Rd}{3} \right) \frac{d^2 \theta_0}{d\eta^2} + -2\chi \theta_0(\eta) + \left(1 - \phi + \phi \frac{(\rho c_p)_s}{(\rho c_p)_f} \right) \left\{ f_0(\eta) \frac{d\theta_0}{d\eta} - 4 \frac{df_0}{d\eta} \theta_0(\eta) \right\} \right] + e^{-\varepsilon \tau} \left[\frac{1}{Pr} \frac{k_{nf}}{k_f} \left(1 + \frac{4Rd}{3} \right) \frac{d^2 G}{d\eta^2} - 2\chi G(\eta, \tau) + \left(1 - \phi + \phi \frac{(\rho c_p)_s}{(\rho c_p)_f} \right) \left\{ f_0(\eta) \frac{dG}{d\eta} + F(\eta, \tau) \frac{d\theta_0}{d\eta} - 4 \frac{df_0}{d\eta} G(\eta, \tau) - 4 \frac{dF}{d\eta} \theta_0(\eta) + 2\tau \varepsilon \frac{df_0}{d\eta} G + \varepsilon G \right\} \right] + e^{-2\varepsilon \tau} \left(1 - \phi + \phi \frac{(\rho c_p)_s}{(\rho c_p)_f} \right) \left[F(\eta, \tau) \frac{dG}{d\eta} - 4 \frac{dF}{d\eta} G(\eta, \tau) + 2\tau \varepsilon \frac{dF}{d\eta} G \right] = 0$$

This implies that

$$\frac{1}{Pr} \frac{k_{nf}}{k_f} \left(1 + \frac{4Rd}{3} \right) \frac{d^2 G}{d\eta^2} + \left(1 - \phi + \phi \frac{(\rho c_p)_s}{(\rho c_p)_f} \right) \left\{ f_0(\eta) \frac{dG}{d\eta} + F(\eta, \tau) \frac{d\theta_0}{d\eta} - 4 \frac{df_0}{d\eta} G(\eta, \tau) - 4 \frac{dF}{d\eta} \theta_0(\eta) + 2\tau \varepsilon \frac{df_0}{d\eta} G + \varepsilon G \right\} - 2\chi G = 0$$

To obtain the steady state solution taking $\tau = 0$, it is obtained

$$\frac{1}{Pr} \frac{k_{nf}}{k_f} \left(1 + \frac{4Rd}{3} \right) G'' + \left(1 - \phi + \phi \frac{(\rho c_p)_s}{(\rho c_p)_f} \right) \left\{ f_0 G'_0 + F_0 \theta'_0 - 4f'_0 G_0 - 4F'_0 \theta_0 + \varepsilon G_0 \right\} - 2\chi G_0 = 0 \quad (B. 20)$$

Now the transformation of boundary conditions in stability analysis of the energy equation

$$\theta(0, \tau) = 1 + \delta_\tau \frac{\partial \theta(0, \tau)}{\partial \eta}$$

Therefore,

$$\theta(0, \tau) = 1 + \delta_\tau \frac{\partial \theta(0, \tau)}{\partial \eta}$$

$$\theta_0(0) + e^{-\varepsilon\tau} G(0, \tau) = 1 + \delta_\tau \left(\frac{d\theta_0(0)}{d\eta} + e^{-\varepsilon\tau} \frac{dG(0, \tau)}{d\eta} \right)$$

$$1 + \delta_\tau \frac{d\theta_0}{d\eta} + e^{-\varepsilon\tau} G(0, \tau) = 1 + \delta_\tau \frac{d\theta_0}{d\eta} + e^{-\varepsilon\tau} \delta_\tau \frac{dG(0, \tau)}{d\eta}$$

$$e^{-\varepsilon\tau} G(0, \tau) = e^{-\varepsilon\tau} \delta_\tau \frac{dG(0, \tau)}{d\eta}$$

By taking $\tau = 0$, we have

$$G(0) = \delta_\tau G'_0(0)$$

$$\theta(\eta, \tau) \rightarrow 0; \quad \text{as } \eta \rightarrow \infty$$

$$\theta_0(\eta) + e^{-\varepsilon\tau} G(\eta, \tau) \rightarrow 0$$

By taking $\tau = 0$, we have

$$0 + e^{-\varepsilon\tau} G_0(\eta, 0) \rightarrow 0$$

$$G_0(\eta) \rightarrow 0; \quad \text{as } \eta \rightarrow \infty$$

Therefore, the required momentum and heat transfer equations for stability analysis are

$$\left(1 + \frac{1}{\beta}\right) F_0'''' + (1 - \phi)^{2.5} \left[\left(1 - \phi + \phi \left(\frac{\rho_s}{\rho_f}\right)\right) (f_0 F_0'' + F_0 f_0'' - 4f_0' F_0' + \varepsilon F_0') \right. \\ \left. + 2\zeta \left(1 - \phi + \phi \frac{(\rho\beta_T)_s}{(\rho\beta_T)_f}\right) G_0 \right] = 0 \quad (B.21)$$

$$\left(1 + \frac{4Rd}{3}\right) G_0'' + Pr \frac{k_f}{k_{nf}} \left[\left(1 - \phi + \phi \frac{(\rho c_p)_s}{(\rho c_p)_f}\right) \{f_0 G_0' + F_0 \theta_0' - 4f_0' G_0 - 4F_0' \theta_0 \right. \right. \\ \left. \left. + \varepsilon G_0\} - 2\chi G_0 \right] = 0 \quad (B.22)$$

Subject to the boundary conditions

$$F_0(0) = 0, \quad F_0'(0) = \delta F_0''(0), \quad G_0(0) = \delta_T G_0'(0) \\ F_0'(\eta) \rightarrow 0, \quad G_0(\eta) \rightarrow 0 \text{ as } \eta \rightarrow \infty \quad (B.23)$$

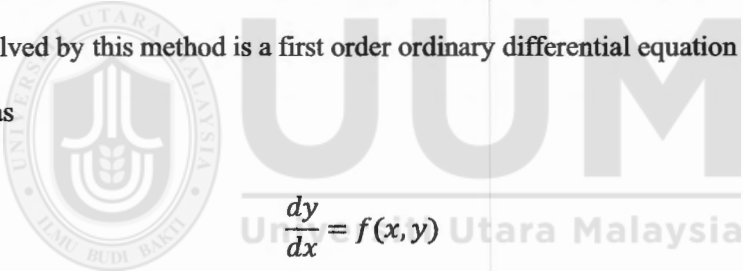
APPENDIX C

RUNGE-KUTTA FOURTH ORDER AND NEWTON-RAPHSON METHOD

In Appendix C, there has been provided a Runge-Kutta method of the order four in Section C.1 and the Newton Raphson method in Section C.2 generally. The detailed explanation of this method can be seen in books by Roberts and Shipman (1972), Fox and Mayers (1990), Jaluria and Torrance (2003) and Greenspan (2006)

C.1 Runge-Kutta fourth order method

This is an important numerical method which is used to solve the differential equations, particularly, higher order ordinary differential equations. The basic differential equation solved by this method is a first order ordinary differential equation which can be written as


$$\frac{dy}{dx} = f(x, y)$$

The dependent variable $y(x)$ can be determined over the given interval $[a, b]$ when the value of the dependent variable y at $x = a$ is given. The classical fourth order Runge-Kutta formula can be written as

$$y_{n+1} = y_n + \frac{1}{6}(S_1 + 2S_2 + 2S_3 + S_4)$$

where

$$S_1 = f(x_n, y_n)\Delta x$$

$$S_2 = f\left(x_n + \frac{\Delta x}{2}, y_n + \frac{S_1}{2}\right)\Delta x$$

$$S_3 = f\left(x_n + \frac{\Delta x}{2}, y_n + \frac{S_2}{2}\right) \Delta x$$

$$S_4 = f(x_n + \Delta x, y_n + S_3) \Delta x$$

Thus, the dependent variable y is determined at x_{n+1} for the given value of x_n and Δx is the increment in x for the determination of y at various value of x . The corresponding expressions for second and third-order approximation may similarly be obtained. Therefore, y is obtained through the approximation of the function $f(x, y)$ at a given number of positions, followed by a suitable weighted averaging.

In same manner, for the higher order equations, simultaneous type of the first order equations are obtained. The second order ordinary differential equations lead us to two first order differential equations, likewise third order ordinary differential equations lead us to three first order differential equations and so on. The two first order equations from the second order ordinary differential equations are written in general form as:

$$\frac{dy^*}{dx} = f(x, y^*, z)$$

and

$$\frac{dz}{dx} = g(x, y^*, z)$$

The solution is written as

$$y_{n+1}^* = y_n^* + \frac{S_1 + 2S_2 + 2S_3 + S_4}{6}$$

and

$$z_{n+1} = z_n + \frac{L_1 + 2L_2 + 2L_3 + L_4}{6}$$

where

$$S_1 = f(x_n, y_n^*, z_n)\Delta x$$

$$L_1 = g(x_n, y_n^*, z_n)\Delta x$$

$$S_2 = f\left(x_n + \frac{\Delta x}{2}, y_n^* + \frac{S_1}{2}, z_n + \frac{L_1}{2}\right)\Delta x$$

$$L_2 = g\left(x_n + \frac{\Delta x}{2}, y_n^* + \frac{S_1}{2}, z_n + \frac{L_1}{2}\right)\Delta x$$

$$S_3 = f\left(x_n + \frac{\Delta x}{2}, y_n^* + \frac{S_2}{2} + z_n + \frac{L_2}{2}\right)\Delta x$$

$$L_3 = g\left(x_n + \frac{\Delta x}{2}, y_n^* + \frac{S_2}{2} + z_n + \frac{L_2}{2}\right)\Delta x$$

$$S_4 = f(x_n + \Delta x, y_n^* + S_3, z_n + L_3)\Delta x$$

$$L_4 = g(x_n + \Delta x, y_n^* + S_3, z_n + L_3)\Delta x$$

The y_n^* and z_n are determined at x_{n+1} for the given value of x_n . Therefore, y^* and z are needed at the initial point, let $x = 0$, to achieve the solution. It should be remembered that higher order differential equations follow the same procedure.

C.2 Newton Raphson method

One of the widely used iterative method for determining the roots of the nonlinear equations such as $f(z) = 0$ is Newton Raphson method. This is one of the flexible and

fast method. This method starts with an initial guess for the root and generates a series of the approximations that is written as

$$z_{n+1} = z_n - \frac{f(z_n)}{f'(z_n)}$$

Where z_{n+1} and z_n are the approximations to the root at the $n + 1$ th and n th iterations, respectively and $f'(z_n)$ is derivative of the $f(z)$ at $z = z_n$. The convergence is assumed if $|f(z_n)| \leq \varepsilon$, where ε is a chosen convergence parameter.



UUM
Universiti Utara Malaysia

APPENDIX D

MAPLE PROGRAM

This maple program solves the problem of steady mixed convection boundary layer flow of Casson based nanofluid over an exponentially shrinking/stretching vertical sheet with effects of suction and the partial slip conditions.

```
> restart ;
> Shootlib := "D:\nanofluid/";
Shootlib := "D:\nanofluid/"
> libname := Shootlib, libname;
libname := "D:\nanofluid/", "C:\Program Files\Maple 18\lib", "."
> with( Shoot );
[shoot]

> with( plots ) :
> S := 6;  $\beta$  := 2.5;  $\Phi$  := 0.1;  $\rho_s$  := 2701;  $\rho_f$  := 989;  $\beta_s$  := 2.31;  $\beta_f$ 
:= 0.99;  $k_s$  := 237;  $k_f$  := 0.6376;  $c_p$  := 902;  $c_{pf}$  := 4175;  $Pr$ 
:= 1.5;  $\zeta$  := 1;  $\chi$  := 0.1;  $\lambda$  := 1.2;  $\delta T$  := 0.1;  $\delta$  := 0.1;  $Rd$ 
:= 0.5;
```

```
S := 6
 $\beta$  := 2.5
 $\Phi$  := 0.1
 $\rho_s$  := 2701
 $\rho_f$  := 989
 $\beta_s$  := 2.31
 $\beta_f$  := 0.99
 $k_s$  := 237
 $k_f$  := 0.6376
 $c_p$  := 902
 $c_{pf}$  := 4175
 $Pr$  := 1.5
 $\zeta$  := 1
 $\chi$  := 0.1
 $\lambda$  := 1.2
 $\delta T$  := 0.1
 $\delta$  := 0.1
 $Rd$  := 0.5
```

$$\begin{aligned}
 > A1 := (1 - \Phi)^{2.5}; A2 := \left((1 - \Phi) + \Phi \cdot \left(\frac{\rho s}{\rho f} \right) \right); A3 := \left((1 - \Phi) \right. \\
 & \quad \left. + \Phi \cdot \left(\frac{\rho s \cdot \beta s}{\rho f \cdot \beta f} \right) \right); A4 := \frac{(k s + 2 \cdot k f - 2 \cdot \Phi \cdot (k f - k s))}{(k s + 2 \cdot k f + \Phi \cdot (k f - k s))}; A5 \\
 & := \left((1 - \Phi) + \Phi \cdot \left(\frac{\rho s \cdot c p s}{\rho f \cdot c p f} \right) \right);
 \end{aligned}$$

A1 := 0.7684334714

A2 := 1.173104146

A3 := 1.537243006

A4 := 1.330362764

A5 := 0.9590035783

>

> blt1 := 6; blt2 := 6; blt3 := 6; % boundary layer thicknesses

blt1 := 6

blt2 := 6

blt3 := 6

blt3 := 6

> FNS := {F(η), Fp(η), Fpp(η), θ(η), θp(η)};

FNS := {F(η), Fp(η), Fpp(η), θ(η), θp(η)}

>

$$\begin{aligned}
 ODE := \left\{ \begin{aligned}
 & \text{diff}(F(\eta), \eta) = Fp(\eta), \text{diff}(Fp(\eta), \eta) = Fpp(\eta), \left(1 \right. \\
 & \quad \left. + \frac{1}{\beta} \right) \cdot \text{diff}(Fpp(\eta), \eta) = -2 \cdot \text{zeta} \cdot A1 \cdot A3 \cdot \theta(\eta) + A1 \cdot A2 \cdot (2 \\
 & \quad \cdot Fp(\eta) \cdot Fp(\eta) - F(\eta) \cdot Fpp(\eta)), \text{diff}(\theta(\eta), \eta) = \theta p(\eta), \\
 & \quad \left(\frac{A4}{Pr} \right) \cdot \left(1 + \frac{4 \cdot Rd}{3} \right) \cdot \text{diff}(\theta p(\eta), \eta) = A5 \cdot (4 \cdot Fp(\eta) \cdot \theta(\eta) \\
 & \quad - F(\eta) \cdot \theta p(\eta)) - 2 \cdot \chi \cdot \theta(\eta) \left. \right\};
 \end{aligned}$$

% Reduce the equation to the first order equations

$$ODE := \left\{ 1.400000000 \left(\frac{d}{d\eta} Fpp(\eta) \right) = -2.362537958 \theta(\eta) \right.$$

$$\left. + 1.802904982 Fp(\eta)^2 - 0.9014524912 F(\eta) Fpp(\eta), \right.$$

$$1.478180849 \left(\frac{d}{d\eta} \theta p(\eta) \right) = 3.836014313 Fp(\eta) \theta(\eta)$$

$$- 0.9590035783 F(\eta) \theta p(\eta) - 0.2 \theta(\eta), \frac{d}{d\eta} F(\eta) = Fp(\eta),$$

$$\left. \frac{d}{d\eta} Fp(\eta) = Fpp(\eta), \frac{d}{d\eta} \theta(\eta) = \theta p(\eta) \right\}$$

$$\begin{aligned}
 > ICI := \{F(0) = S, Fpp(0) = \alpha, Fp(0) = \lambda + \delta \cdot \alpha, \theta p(0) = \psi, \theta(0) \\
 & = 1 + \delta T \cdot \psi \};
 \end{aligned}$$

% Initial conditions

$IC1 := \{F(0) = 6, Fp(0) = 0.1 \alpha + 1.2, Fpp(0) = \alpha, \theta(0) = 0.1 \psi + 1, \theta p(0) = \psi\}$

> $BC1 := \{Fp(blt1) = 0, \theta(blt1) = 0\}; BC2 := \{Fp(blt2) = 0, \theta(blt2) = 0\}; BC3 := \{Fp(blt3) = 0, \theta(blt3) = 0\}$

% Boundary conditions

$BC1 := \{Fp(6) = 0, \theta(6) = 0\}$

$BC2 := \{Fp(6) = 0, \theta(6) = 0\}$

$BC3 := \{Fp(6) = 0, \theta(6) = 0\}$

> $infolevel[shoot] := 1 :$

> $S1 := shoot(ODE, IC1, BC1, FNS, [\alpha = -3.2777190862989807, \psi = -2.9666488119981618,])$:

shoot: Step # 1

shoot: Parameter values : alpha = -3.2777190862989807 psi = -2.9666488119981618

> $W1 := shoot(ODE, IC1, BC2, FNS, [\alpha = -10.374753017708157, \psi = -10.159231645187077,])$:

shoot: Step # 1

shoot: Parameter values : alpha = -10.374753017708157 psi = -10.159231645187077

> $M1 := shoot(ODE, IC1, BC3, FNS, [\alpha = -11.036513337814583, \psi = -2.123167944078309])$:

shoot: Step # 1

shoot: Parameter values : alpha = -11.036513337814583 psi = -2.123167944078309

> $p1 := odeplot(S1, [\eta, Fp(\eta)], 0 ..blt1, numpoints = 500, color = blue)$:

> $p2 := odeplot(S1, [\eta, \theta(\eta)], 0 ..blt1, numpoints = 500, color = blue)$:

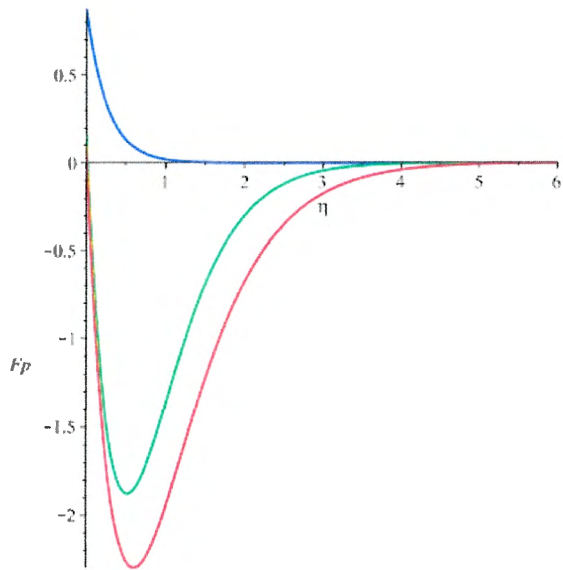
> $w1 := odeplot(W1, [\eta, Fp(\eta)], 0 ..blt2, numpoints = 500, color = green)$:

> $w2 := odeplot(W1, [\eta, \theta(\eta)], 0 ..blt2, numpoints = 500, color = green)$:

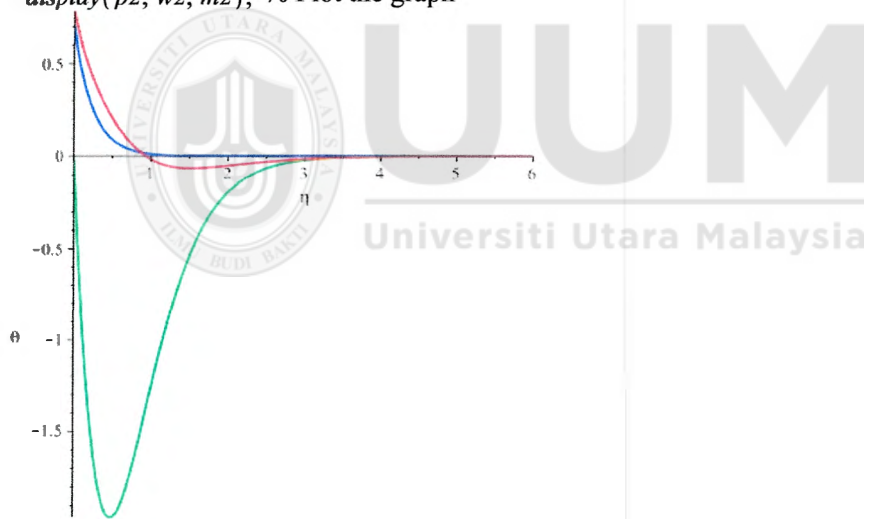
> $m1 := odeplot(M1, [\eta, Fp(\eta)], 0 ..blt3, numpoints = 500)$:

> $m2 := odeplot(M1, [\eta, \theta(\eta)], 0 ..blt3, numpoints = 500)$:

> $display(p1, w1, m1);$ % Plot the graph



`> display(p2, w2, m2); % Plot the graph`



APPENDIX E

MATLAB PROGRAM FOR THE STABILITY ANALYSIS

This MATLAB program solves the problem of steady laminar incompressible boundary layer flow of Aluminum Casson based nanofluid in an exponentially vertical stretching/shrinking sheet with the help of 3-Stage Lobatto III-A Formula:

- First Program for the first solution

```
function Casson_1st_solution;
clear all;
clc;
global beta lambda A1 Pr chi zeta deltaT Rd A3 A2 A4 A5 phi ros rof ks kf cps cpf S Bos Bof

beta=2.5; lamda=1.2; Pr=1.5; phi=0.1; ros=2701; rof=989; Bos=2.31; Bof=0.99; ks=237; kf=0.6376;
cps=902; cpf=4175; chi=0.1; zeta=1; delta=0.1; deltaT=0.1; Rd=0.5; S=6;

A1=((1-phi)^2.5);
A2=((1-phi)+phi*(ros/rof));
A3= (1-phi)+phi*((ros*cps)/(rof*cpf));
A4 = (ks+2*kf-2*phi*(kf-ks))/(ks+2*kf+phi*(kf-ks));
A5= (1-phi)+phi*((ros*Bos)/(rof*Bos));

a = 0; % for the initial conditions
b =6; % For the boundary conditions
solinit = bvpinit(linspace(a,b,30),@guess);
options = bvpset('stats','on','RelTol',1e-7);
sol = bvp4c(@Tiwari_ode,@Tiwari_bc,solinit,options);

figure (1)
plot(sol.x,sol.y(2,:), 'b')
xlabel('\eta')
ylabel ('f'(\eta))
hold on

figure (2)
```

```

plot(sol.x,sol.y(4,:),r')
xlabel('\eta')
ylabel('\theta(\eta)')
hold on
descrip=[sol.x; sol.y];
save 'first_sol_Casson.txt' descrip -ascii
fprintf('skin friction = %7.9f.\n', sol.y(3,2));
fprintf('heat transfer rate = %7.9f.\n', sol.y(5,1));
%-----

function dydx = Tiwari_ode(x,y,beta,A1,Pr,A3,A2,A4,A5,Rd,chi,zeta)
global beta A4 A5 A1 Pr A3 A2 Rd chi zeta
dydx = [y(2)
        y(3)
        ((beta/(1+beta))*(-2*A1*A5*zeta*y(4)+2*A1*A2*y(2)*y(2)-A1*A2*y(3)*y(1)))
        y(5)
        (((3/(3+4*Rd))*(Pr/A4)*(-2*chi*y(4)+4*A3*y(4)*y(2)-A3*y(5)*y(1))))];
%-----

function BC = Tiwari_bc(ya,yb,lamda,S,delta,deltaT)
global S delta deltaT lamda
BC = [ya(1)-S
      ya(2)-lamda-delta*ya(3)
      yb(2)
      ya(4)-1-deltaT*ya(5)
      yb(4)];
%-----

function v = guess (x,fw, lambda)
global S lambda
v = [S
      lambda
      0
      1
      0];

```

After command, conclusion:

The solution was obtained on a mesh of 126 points.

The maximum residual is 9.866e-08.

There were 6314 calls to the ODE function.

There were 129 calls to the BC function.

skin friction = -3.249492924.

heat transfer rate = -2.964170805.

- Second program for the second solution

```
function Casson_2nd_solution;
clear all;
clc;
global beta lambda A1 Pr chi zeta delta deltaT Rd A3 A2 A4 A5 phi ros rof ks kf cps cpf S Bos Bof
beta=2.5; lambda=1.2; Pr=1.5; phi=0.1; ros=2701; rof=989; Bos=2.31; Bof=0.99; ks=237; kf=0.6376;
cps=902; cpf=4175; zeta=1; chi=0.1; delta=0.1; deltaT=0.1; Rd=0.5; S=6;

A1=((1-phi)^2.5);
A2=((1-phi)+phi*(ros/rof));
A3=(1-phi)+phi*((ros*cps)/(rof*cpf));
A4=(ks+2*kf-2*phi*(kf-ks))/(ks+2*kf+phi*(kf-ks));
A5=(1-phi)+phi*((ros*Bos)/(rof*Bos));

a = 0; % for the initial conditions
b = 6; % For the boundary conditions

solinit = bvpinit(linspace(a,b,13),@guess);
options = bvpset('stats','on','RelTol',1e-5);
sol = bvp4c(@Tiwari_ode,@Tiwari_bc,solinit,options);

figure(1)
plot(sol.x,sol.y(2,:), 'b')
xlabel('\eta')
ylabel('f'(\eta))
hold on

figure(2)
plot(sol.x,sol.y(4,:), 'r')
xlabel('\eta')
ylabel('\theta(\eta)')
hold on
descrip=[sol.x; sol.y];
```

```

save 'second_sol_Casson.txt' describ -ascii
fprintf('skin friction = %7.9f.\n', sol.y(3,1));
fprintf('heat transfer rate = %7.9f.\n', sol.y(5,4));
%-----

function dydx = Tiwari_ode(x,y,beta,A1,Pr,A3,A2,A4,A5,Rd,chi,zeta)
global beta A4 A5 A1 Pr A3 A2 Rd chi zeta
dydx = [y(2)
        y(3)
        ((beta/(1+beta))*(-2*A1*A5*zeta*y(4)+2*A1*A2*y(2)*y(2)- 1*A2*y(3)*y(1)))
        y(5)
        (((3/(3+4*Rd))*(Pr/A4)*(-2*chi*y(4)+4*A3*y(4)*y(2)-A3*y(5)*y(1))))];
%-----

function BC = Tiwari_bc(ya,yb,lambda,S,delta,deltaT)
global S delta deltaT lambda
BC = [ya(1)-S
      ya(2)-lambda-delta*ya(3)
      yb(2)
      ya(4)-1-deltaT*ya(5)
      yb(4)];
%-----

function v = guess(x,S)
global S
v = [exp(-x)
     exp(-0.1*x)
     sin(-x)
     exp(-x)
     cos(x)-2];

```

After command, conclusion:

The solution was obtained on a mesh of 325 points.

The maximum residual is 9.649e-06.

There were 12056 calls to the ODE function.

There were 222 calls to the BC function.

skin friction = -10.417543960.

heat transfer rate = -10.183627818.

- Third program for the third solutions

```

function Casson_3rd_solution;
clear all;
clc;
global beta lambda A1 Pr zeta chi delta deltaT Rd A3 A2 A4 A5 phi ros rof ks kf cps cpf S Bos Bof

beta=2.5; lamda=1.2; Pr=1.5; phi=0.1; ros=2701; rof=989; Bos=2.31; Bof=0.99; ks=237; kf=0.6376;
cpf=902; cps=4175; zeta=1; chi=0.1; delta=0.1; deltaT=0.1; Rd=0.5; S=6;

A1=((1-phi)^2.5);
A2=((1-phi)+phi*(ros/rof));
A3= (1-phi)+phi*((ros*cps)/(rof*cpf));
A4 = (ks+2*kf-2*phi*(kf-ks))/(ks+2*kf+phi*(kf-ks));
A5= (1-phi)+phi*((ros*Bos)/(rof*Bos));

a = 0; % for the initial conditions
b = 6; % For the boundary conditions

solinit = bvpinit(linspace(a,b,13),@guess);
options = bvpset('stats','on','RelTol',1e-6);
sol = bvp4c(@Tiwari_ode,@Tiwari_bc,solinit,options);

figure(1)
plot(sol.x,sol.y(2,:), 'b')
xlabel('\eta')
ylabel ('f'(\eta))
hold on

figure(3)
plot(sol.x,sol.y(4,:), 'r')
xlabel('\eta')
ylabel('\theta(\eta)')
hold on
descrip=[sol.x; sol.y];
save '3rd_sol_Casson.txt' descrip -ascii
fprintf('skin friction = %7.9f.\n', sol.y(3,1));
fprintf('heat transfer rate = %7.9f.\n', sol.y(5,1));
%-----
function dydx = Tiwari_ode(x,y,beta,A1,Pr,A3,A2,A4,A5,Rd,zeta,chi)
global beta A4 A5 A1 Pr A3 A2 R gamma xi
dydx = [y(2)

```

```

y(3)
((beta/(1+beta))*(-2*A1*A5*zeta*y(4)+2*A1*A2*y(2)*y(2)-A1*A2*y(3)*y(1)))
y(5)
(((3/(3+4*Rd))*(Pr/A4)*(-2*chi*y(4)+4*A3*y(4)*y(2)-A3*y(5)*y(1)))));
%-----
function BC = Tiwari_bc(ya,yb,lambda,S,delta,deltaT)
global S c1 c2 lamda
BC = [ya(1)-S
      ya(2)-lambda-delta*ya(3)
      yb(2)
      ya(4)-1-deltaT*ya(5)
      yb(4)];
%-----
function v = guess(x,S)
global S
v = [cos(-x)
      exp(-0.1*x)
      0.1+sin(-x)
      exp(-2*x)
      cos(x)-23];

```

After command, conclusion:

The solution was obtained on a mesh of 261 points.

The maximum residual is 9.743e-07.

There were 16124 calls to the ODE function.

There were 247 calls to the BC function.

skin friction = -11.216626785.

heat transfer rate = -2.100149313.

- Fourth Program for the velocity's profiles combinedly.

```

function Tri_Casson_velocity;
clc
clear
format long g
global lamda S A1 Pr zeta chi delta deltaT Rd A3 A2 A4 A5 phi ros rof ks kf cps cpf Bos Bof

lamda=1.2; S=6; Pr=1.5; phi=0.1; ros= 2701; rof=989;Bos=2.31;Bof=0.99;
ks=237; kf=0.6376; cps=902; cpf=4175; zeta=1; chi=0.1; delta=0.1; deltaT=0.1; Rd=0.5;

A1=((1-phi)^2.5);
A2=((1-phi)+phi*(ros/rof));
A3= (1-phi)+phi*((ros*cps)/(rof*cpf));
A4 = (ks+2*kf-2*phi*(kf-ks))/(ks+2*kf+phi*(kf-ks));

```

```

A5= (1-phi)+phi*((ros*Bos)/(rof*Bos));

% 1st

for beta=2.5:0.01:2.8
if beta == 2.5
    lo=load('first_sol_Casson.txt');
    solinit.x=lo(1,:);solinit.y=lo(2:6,:);
else
    solinit.x = sol.x; solinit.y=sol.y;
end

options = bvpset('stats','off','RelTol',1e-10);
sol =bvp4c(@Tiwari_ode,@Tiwari_bc,solinit,options);

end

figure(1)
plot(sol.x,sol.y(2,:), 'k:')
hold on

figure(2)
plot(sol.x,sol.y(4,:), 'k:')
hold on

save ('casson_first_solution.mat', '-struct', 'sol');

% 2nd

for beta=2.5:0.01:2.8
if beta == 2.5
    lo=load('second_sol_Casson.txt');
    solinit.x=lo(1,:);solinit.y=lo(2:6,:);
else
    solinit.x = sol.x; solinit.y=sol.y;
end

options = bvpset('stats','off','RelTol',1e-10);
sol = bvp4c(@Tiwari_ode,@Tiwari_bc,solinit,options);

end

figure(1)
plot(sol.x,sol.y(2,:), 'k:')
hold on
figure(2)
plot(sol.x,sol.y(4,:), 'k:')
hold on

save ('casson_second_solution.mat', '-struct', 'sol');

% 3rd

for beta=2.5:0.01:2.8
if beta == 2.5
    lo=load('3rd_sol_Casson.txt');
    solinit.x=lo(1,:);solinit.y=lo(2:6,:);

```

```

else
    solinit.x = sol.x; solinit.y=sol.y;
end

options = bvpset('stats','off','RelTol',1e-10);
sol = bvp4c(@Tiwari_ode,@Tiwari_bc,solinit,options);

end

figure(1)
plot(sol.x,sol.y(2,:), 'k')
hold on

figure(2)
plot(sol.x,sol.y(4,:), 'k')
hold on

save ('casson_third_solution.mat', '-struct', 'sol');

% -----
function dydx = Tiwari_ode(x,y,beta,A1,Pr,A3,A2,A4,A5,Rd,zeta,chi)
global beta A4 A5 A1 Pr A3 A2 R gamma xi
dydx = [y(2)
        y(3)
        ((beta/(1+beta))*(-2*A1*A5*zeta*y(4)+2*A1*A2*y(2)*y(2)-A1*A2*y(3)*y(1)))
        y(5)
        (((3/(3+4*Rd))*(Pr/A4)*(-2*chi*y(4)+4*A3*y(4)*y(2)-A3*y(5)*y(1))))];
% -----
function BC = Tiwari_bc(ya,yb,lambda,S,delta,deltaT)
global fw c1 c2 lambda
BC = [ya(1)-S
      ya(2)-lambda-delta*ya(3)
      yb(2)
      ya(4)-1-deltaT*ya(5)
      yb(4)];
% -----
function v = guess(x,S)
global S
v = [1+x
     -1
     1-exp(-x)
     1
     1+cos(x)];

```

- Fifth program for the stability of the first solution

```

function Casson_1st_stability;
format long g
clear all;
clc;
global beta lamda A1 Pr epsilon chi delta deltaT Rd A3 A2 A4 A5 phi ros rof ks kf cps cpf S Bos Bof
zeta D

beta=2.5; lambda=1.2; Pr=1.5; phi=0.1; ros=2701; rof=989; Bos=2.31; Bof=0.99;ks=237; kf=0.6376;
cps=902; cpf=4175; zeta=1; chi=0.1; delta=0.1; deltaT=0.1; Rd=0.5; S=6;

A1=((1-phi)^2.5);

```

```

A2=((1-phi)+phi*(ros/rof));
A3= (1-phi)+phi*((ros*cps)/(rof*cpf));
A4 = (ks+2*kf-2*phi*(kf-ks))/(ks+2*kf+phi*(kf-ks));
A5= (1-phi)+phi*((ros*Bos)/(rof*Bos));
a = 0;
b= 6;

```

```

D = load('casson_first_solution.mat');
err = [];
gam = [];
for epsilon=7.5128:0.0001:7.513
    solinit = bvpinit(linspace(a,b,5),@Tiwari_init);
    options = bvpset('stats','off','RelTol',1e-10);
    sol = bvp4c(@Tiwari_ode,@Tiwari_bc,solinit,options);
    figure(1)
    plot(sol.x,sol.y(2,:), 'r')
    hold on
    plot(sol.x,sol.y(1,:), 'b')
    hold on
    disp([epsilon,abs(sol.y(4,end))]);
    err = [err,abs(sol.y(4,end))];
    gam = [gam,epsilon];

```

```
end
```

```

figure(2)
plot(gam,err);
min(err)
% figure(3)
% plot(C,epsilon,'r');
% xlabel('c/a')
% ylabel ('epsilon')
hold on
%fprintf('eigen value = %7.3f\n',sol.parameters);
% -----
function dydx = Tiwari_ode(x,y,zeta,D,s,beta,A1,Pr,A3,A2,A4,A5,Rd,epsilon,chi)
global beta A1 Pr A3 A2 A4 A5 Rd epsilon chi zeta D s
[s,sp] = deval(D,x);
dydx = [y(2)
        y(3)
        ((beta/(1+beta))*A1*(A2*(-s(1)*y(3)-s(3)*y(1)+4*s(2)*y(2)-epsilon*y(2))-2*zeta*A5*y(4)))
        y(5)
        ((Pr/A4)*(3/(3+4*Rd))*(A2*(4*s(2)*y(4)+4*y(2)*s(4)-s(1)*y(5)-y(1)*s(4)-
        epsilon*y(4))+2*chi*y(4)))]];
% -----

```

```

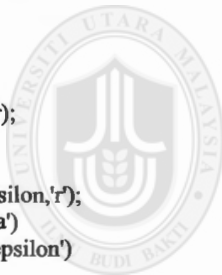
function BC= Tiwari_bc(ya,yb,c1,c2)
global c1 c2
BC = [ ya(1)
        ya(2)-delta*ya(3)
        ya(3)-1
        ya(4)-deltaT*ya(5)
        yb(4)];
% -----

```

```

function v = Tiwari_init(x)
v = [0
      0
      1
      0
      0];

```



UUM
Universiti Utara Malaysia

After command, conclusion:

```
7.5128 5.87464922056469e-36
7.5129 1.05037912929658e-40
7.513 2.05796426525044e-36
```

ans =

```
1.05037912929658e-40
```

- Sixth program for the stability of the second solution

```
function Casson_2nd_stability;
format long g
clear all;
clc;
global beta lamda A1 Pr epsilon chi delta deltaT Rd A3 A2 A4 A5 phi ros rof ks kf cps cpf fw Bos Bof
zeta D
```

```
beta=2.5;lamda=1.2; Pr=1.5; phi=0.1; ros= 2701; rof=989; Bos=2.31; Bof=0.99;ks=237; kf=0.6376;
cps=902; cpf=4175; b1=1; b2=0.1; c1=0.1; c2=0.1; Rd=0.5; S=6;
```

```
A1=((1-phi)^2.5);
A2=((1-phi)+phi*(ros/rof));
A3=(1-phi)+phi*(ros*cps)/(rof*cpf);
A4=(ks+2*kf-2*phi*(kf-ks))/(ks+2*kf+phi*(kf-ks));
A5=(1-phi)+phi*((ros*Bos)/(rof*Bos));
a = 0;
b= 6;
```

```
D = load('casson_second_solution.mat');
err = [];
gam = [];
for epsilon=-7.0012:0.0001:-7.001
    solinit = bvpinit(linspace(a,b,5),@Tiwari_init);
    options = bvpset('stats','off','RelTol',1e-10);
    sol = bvp4c(@Tiwari_ode,@Tiwari_bc,solinit,options);
    figure(1)
    plot(sol.x,sol.y(2,:), 'r')
    hold on
    plot(sol.x,sol.y(1,:), 'b')
    hold on
    disp([epsilon,abs(sol.y(4,end))]);
    err = [err,abs(sol.y(4,end))];
    gam = [gam,epsilon];
end
```

```
figure(2)
plot(gam,err);
```

```

min(err)
% figure(3)
% plot(C, epsilon,'r');
% xlabel('c/a')
% ylabel ('\epsilon')
hold on
%fprintf('eigen value = %7.3f.\n',sol.parameters);
% -----
function dydx = Tiwari_ode(x,y,zeta,D,s,beta,A1,Pr,A3,A2,A4,A5,Rd,epsilon,chi)
global beta A1 Pr A3 A2 A4 A5 R epsilon chi zeta D s
[s,sp] = deval(D,x);
dydx = [y(2)
        y(3)
        ((beta/(1+beta))*A1*(A2*(-s(1)*y(3)-s(3)*y(1)+4*s(2)*y(2)-epsilon*y(2))-2*zeta*A5*y(4)))
        y(5)
        ((Pr/A4)*(3/(3+4*Rd))*(A2*(4*s(2)*y(4)+4*y(2)*s(4)-s(1)*y(5)-y(1)*s(4)-
epsilon*y(4))+2*chi*y(4)))];
% -----
function BC= Tiwari_bc(ya,yb,delta,deltaT)
global delta deltaT
BC = [ ya(1)
        ya(2)-delta*ya(3)
        ya(3)-1
        ya(4)-deltaT*ya(5)
        yb(4)];
% -----
function v = Tiwari_init(x)
v = [0
      0
      1
      0
      0];

```

After command, conclusion:

```

-7.0012    6.4521184175886e-34
-7.0011    7.38782935662613e-35
-7.001    3.36853998929877e-34

```

ans =

```

7.38782935662613e-35

```

- Seventh program for the stability of the second solution

```

function Casson_3rd_stability;
format long g
clear all;
clc;
global beta lamda A1 Pr zeta chi delta deltaT R A3 A2 A4 A5 phi ros rof ks kf cps cpf S Bos Bof epsilon
D

```

```
beta=2; lambda=1; Pr=1.5; phi=0.1; ros= 2701; rof=989; Bos=2.31; Bof=0.99;ks=237; kf=0.6376;
cps=902; cpf=4175; zeta=1; chi=0.1; delta=0.1; deltaT=0.1; Rd=0.5; S=6;
```

```
A1=((1-phi)^2.5);
A2=((1-phi)+phi*(ros/rof));
A3= (1-phi)+phi*((ros*cps)/(rof*cpf));
A4 = (ks+2*kf-2*phi*(kf-ks))/(ks+2*kf+phi*(kf-ks));
A5= (1-phi)+phi*((ros*Bos)/(rof*Bos));
a = 0;
b= 6;
```

```
D = load('casson_third_solution.mat');
err = [];
gam = [];
for epsilon =-5.5622:0.0001:-5.562
    solinit = bvpinit(linspace(a,b,5),@Tiwari_init);
    options = bvpset('stats','off','RelTol',1e-10);
    sol = bvp4c(@Tiwari_ode,@Tiwari_bc,solinit,options);
    figure(1)
    plot(sol.x,sol.y(2,:), 'r')
    hold on
    plot(sol.x,sol.y(1,:), 'b')
    hold on
    disp([epsilon,abs(sol.y(4,end))]);
    err = [err,abs(sol.y(4,end))];
    gam = [gam,epsilon];
end
```

```
figure(2)
plot(gam,err);
min(err)
% figure(3)
% plot(C,epsilon,'r');
% xlabel('c/a')
% ylabel ('\epsilon')
hold on
%fprintf('eigen value = %7.3f.\n',sol.parameters);
% -----
function dydx = Tiwari_ode(x,y,epsilon,D,s,beta,A1,Pr,A3,A2,A4,A5,Rd,zeta,chi)
global beta A1 Pr A3 A2 A4 A5 Rd zeta chi epsilon D s
[s,sp] = deval(D,x);
dydx = [y(2)
        y(3)
        ((beta/(1+beta))*A1*(A2*(-s(1)*y(3)-s(3)*y(1)+4*s(2)*y(2)-epsilon*y(2))-2*zeta*A5*y(4)))
        y(5)
        ((Pr/A4)*(3/(3+4*Rd))*(A2*(4*s(2)*y(4)+4*y(2)*s(4)-s(1)*y(5)-y(1)*s(4)-
epsilon*y(4))+2*chi*y(4)))]];
% -----
function BC= Tiwari_bc(ya,yb,delta,deltaT)
global delta deltaT
BC = [ ya(1)
        ya(2)-delta*ya(3)
        ya(3)-1
        ya(4)-deltaT*ya(5)
        yb(4)];
% -----
function v = Tiwari_init(x)
v = [0
```

```
0
1
0
0];
```

After command, conclusion:

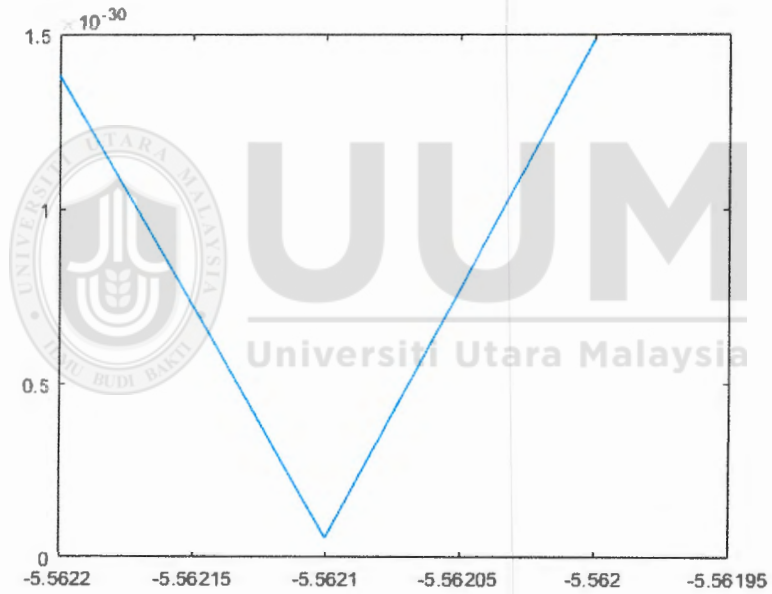
```
-5.5622  1.38398742816368e-30
```

```
-5.5621  5.97849973431726e-32
```

```
-5.562   1.48309437134015e-30
```

ans =

```
5.97849973431726e-32
```



Appendix F

LIST OF PUBLICATIONS

1. Dero, S., Rohni, A. M., Saaban, A., & Khan, I. (2019). Dual Solutions and Stability Analysis of Micropolar Nanofluid Flow with Slip Effect on Stretching/Shrinking Surfaces. *Energies*, 12(23), 4529.
2. Dero, S., Rohni, A. M., & Saaban, A. (2019). MHD micropolar nanofluid flow over an exponentially stretching/shrinking surface: Triple solutions. *J. Adv. Res. Fluid Mech. Therm. Sci*, 56, 165-174.
3. Dero, S., Uddin, M. J., & Rohni, A. M. (2019). Stefan blowing and slip effects on unsteady nanofluid transport past a shrinking sheet: Multiple solutions. *Heat Transfer—Asian Research*, 48(6), 2047-2066.
4. Dero, S., Rohni, A. M., & Saaban, A. 2019. The Dual Solutions and Stability Analysis of Nanofluid Flow using Tiwari-Das Model over a Permeable Exponentially Shrinking Surface with Partial Slip Conditions. *Journal of Engineering and Applied Sciences*, 14: 4569-4582.
DOI: [10.36478/jeasci.2019.4569.4582](https://doi.org/10.36478/jeasci.2019.4569.4582)
5. Dero, S., Mohd Rohni, A., & Saaban, A (2020). Effects of the viscous dissipation and chemical reaction on Casson nanofluid flow over the permeable stretching/shrinking sheet. *Heat Transfer*, 49 (4), 1736 – 1755.
6. Dero, S., Rohni, A. M., & Saaban, A. (2020). Stability analysis of Cu–C₆H₉NaO₇ and Ag– C₆H₉NaO₇ nanofluids with effect of viscous dissipation over stretching and shrinking surfaces using a single phase model. *Heliyon*, 6(3), e03510.
7. Dero, S., Rohni, A.M., & Saaban, A. (2020) Triple Solutions and Stability Analysis of Mixed Convection Boundary Flow of Casson Nanofluid over an

- Exponentially Vertical Stretching/Shrinking Sheet, *J. Adv. Res. Fluid Mech. Therm. Sci.*, (in press).
8. Lund, L. A., Omar, Z., Khan, I., & Dero, S. (2019). Multiple solutions of Cu-C₆H₉NaO₇ and Ag-C₆H₉NaO₇ nanofluids flow over nonlinear shrinking surface. *Journal of Central South University*, 26(5), 1283-1293.
 9. Ghoto, A., Dero, S., Lund, L., Kamboh, S., Memon, K., & Sheikh, A. (2019). Slip effects on Magnetohydrodynamic (MHD) flow of Williamson Nanofluid over an Exponentially Shrinking Sheet. *Sindh University Research Journal-SURJ (Science Series)*, 51(3), 519-526.
 10. Lund, L. A., Omar, Z., Dero, S., & Khan, I. (2020). Linear stability analysis of MHD flow of micropolar fluid with thermal radiation and convective boundary condition: Exact solution. *Heat Transfer—Asian Research*, 49(1), 461-476.
 11. Yan, L., Dero, S., Khan, I., Mari, I. A., Baleanu, D., Nisar, K. S., ... & Abdo, H. S. (2020). Dual Solutions and Stability Analysis of Magnetized Hybrid Nanofluid with Joule Heating and Multiple Slip Conditions. *Processes*, 8(3), 332.